Institutionen för systemteknik
Department of Electrical Engineering

Examensarbete

Simulation and Analysis of a Continuously Variable Cam Phasing Internal Combustion Engine

Examensarbete utfört i Vehicular Systems
vid Tekniska högskolan i Linköping
av

Pär Hammarlund

LITH-ISY-EX--08/4078--SE

Linköping 2008

Simulation and Analysis of a Continuously Variable Cam Phasing Internal Combustion Engine

Examensarbete utfört i Vehicular Systems
vid Tekniska högskolan i Linköping
av

Pär Hammarlund

LITH-ISY-EX--08/4078--SE

Handledare: **Per Öberg**
ISY, Linköpings universitet

Examinator: **Associate Professor Lars Eriksson**
ISY, Linköpings universitet

Linköping, 12 June, 2008

Titel
Title

Simulering och analys av en förbränningsmotor med kontinuerligt varierbar kamaxelfasning

Simulation and Analysis of a Continuously Variable Cam Phasing Internal Combustion Engine

Författare
Author

Pär Hammarlund

Sammanfattning
Abstract

The development of fuel efficient internal combustion engines (ICE) have resulted in a variety of different solutions. One of those are the variable valve timing and an implemenation of such is the Continuously Variable Cam Phasing (CVCP). This thesis have used a simulation package, psPack, for the simulation of the gas exchange process for an ICE with CVCP. The purpose of the simulations was to investigate what kind of design parameters, e.g. the length of an intake pipe or the duration of combustion, that were significant for the gas exchange process with the alternation of intake pressure, engine speed and valve setting. The parameters that showed a vast impact were those who affected the amount of residual gas and the temperature of the air charge.

Furthermore a validation was made between simulation data acquired from psPack and measured data provided in Heywood (1988). The validation showed that for the general behaviour the simulation results from psPack corresponded well to the measured data.

Abstract

The development of fuel efficient internal combustion engines (ICE) have resulted in a variety of different solutions. One of those are the variable valve timing and an implemenation of such is the Continuously Variable Cam Phasing (CVCP). This thesis have used a simulation package, psPack, for the simulation of the gas exchange process for an ICE with CVCP. The purpose of the simulations was to investigate what kind of design parameters, e.g. the length of an intake pipe or the duration of combustion, that were significant for the gas exchange process with the alternation of intake pressure, engine speed and valve setting. The parameters that showed a vast impact were those who affected the amount of residual gas and the temperature of the air charge.

Furthermore a validation was made between simulation data acquired from psPack and measured data provided in Heywood (1988). The validation showed that for the general behaviour the simulation results from psPack corresponded well to the measured data.

Acknowledgments

Contents

Chapter 1

Introduction

A short introduction for this thesis is given, and the concepts of a four-stroke engine and CVCP are introduced.

1.1 Background

With the growing concern on enviromental issues caused by combustion engines, a more fuel efficient engine is wanted. Over the last two decades a large number of solutions have been made for the internal combustion engine making it more efficient. A couple of these solutions have been fuel injection (in-cylinder or port injection), supercharging and downsizing (turbocharger or supercharger) and recently also available for a greater mass production, Variable Valve Timing (VVT) or Variable Cam Timing (VCT). One technique for the variable valve timing is the *Continuosly Variable Cam Phasing* (CVCP).

The main reference in this thesis is John B. Heywood's "Internal Combustion Engine Fundamentals" ([4]). Therefore, some figures presented in [4] have been used as a comparison with results gathered from this thesis.

1.2 Four-Stroke Engine

This thesis is focused on four-stroke engines[1] and how their gas exchange processes work. A four-stroke engine incorporates four different strokes, or phases; the intake, compression, combustion and the exhaust phase.

The gas exchange process occurs during the exhaust and intake strokes, i.e. the removal of exhaust gas and the filling of air/fuel mixture, in the cylinder.

---

[1]when spoken of "engine", the internal combustion engine (ICE) is omitted (in this thesis), thus *engine* will be short for ICE unless stated elsewise.

With various type of valve settings (i.e. valve opening/closing/overlap and duration) the gas exchange process can be vastly influenced.

1.3   Continuously Variable Cam Phasing, CVCP, Basics

The CVCP application in an internal combustion engine works in the way that it rotates, or phases, the camshaft relative to the camshaft sprocket. This will let the camshaft sprocket (which is connected to the cranskhaft via a (drive)chain or a timing belt) to turn without turning the camshaft. Therefore, it is possible to alter the phasing of the valve profile (i.e.. the opening/closing of the valve). With a dual overhead camshaft, both the intake -and exhaust camshaft could be set independently of one another. The number of valve settings, i.e. the degree of freedom for camshaft phasing, are set by design criterion. With a shift of valve settings, the influence on the amount of air/fuel mixture (air charge) and residual gas[2] are two important factors. The air charge is important for fuel and torque control and the residual gas for its effect on engine operation.

If the intake valve opens at an early crank angle, with the exhaust valve still opened, the pumping of the exhaust gas is in full due. At a fired cycle the exhaust gas, which (more often than not) will be at higher pressure than that of the air in the intake manifold, will expand into the same. This will lead to an increase on the amount of residual gas for the next cycle.

The valve setting described in the paragraph above is said to have a nonzero valve overlap. This valve setting is most favored at high intake pressures and high engine speed, i.e. at vast mass flows. It will aid the scavenging of exhaust gas in the cylinder and thus minimise the amount of residual gas. (This in turn can produce some unburned hydrocarbons (HC) in the exhaust. Hence, the amount of inducted air in the cylinder during the intake phaes will increase. Thus, the amount of energy for combustion will increase.)

With the opposite valve setting, i.e. no valve overlap, the expansion of exhaust gas into the intake pipe is reduced. (Residual gas can still expand into the intake pipe.) Therefore this valve setting can be used at low intake pressures and engine speeds.

1.4   psPack

The simulation model used in this thesis has been implemented in MATLAB SIMULINK. The model, called *psPack* ([8]), has been (and is still being), developed by Per Öberg at Vehicular Systems. The model will be further introduced in Chapter 3.

---

[2]the amount of exhaust gas trapped inside the cylinder when the exhaust valve closes (EVC), is referred to as residual gas.
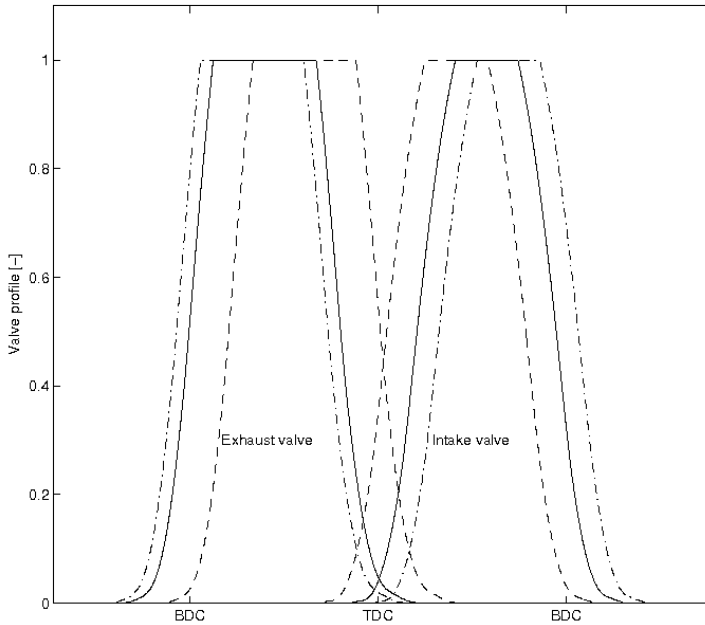
Figure 1.1. Different valve profiles plotted against crank angles. The valve overlap occurs during those crank angles where both the exhaust valve (EV) and the intake valve (IV) is opened.

1.5   Objective

The objective with this thesis was to investigate what kind of design parameters that are significant for the gas exchange process. The different design parameters used in this thesis are described further in Chapter 5, an example of such a design parameter is the length of an intake pipe. In addition, why and how these parameters[3] affect the gas exchange process at different operation points, should be investigated. Furthermore, the value of each parameter was changed by $\pm$ 5% from its nominal value. Parameters corresponding to pipes and etcetera, that are located before the intake manifold, or after the exhaust manifold, will not be investigated.

---

[3] when spoken of the design parameters that have had their values altered, the part "design" in design paramter will be omitted.

The three parameters $Duration$, i.e burn duration, $Phasing$, i.e the crank angle at which 50% of the total mass inside the cylinder has burned, and T_{Wall}, i.e the cylinder wall temperature, were the only parameters that can change from cycle to cycle or within a cycle, during the operation of an engine. With the exception of these parameters, the chosen parameters that were used in this thesis for the sensitivity analysis, corresponds to areas or lengths for different pipes/volumes or valves.

The trustworthiness of psPack should also be confirmed with a comparison between measured data and simulation results.

Chapter 2

Ideal Otto Cycle and Heat Transfer

In this chapter some important properties of heat transfer and an expression for the residual gas mass fraction from the ideal Otto cycle, will be presented.

2.1 Ideal Otto

The ideal Otto cycle is presented and explained further in several references see e.g. [6], [4], or [1]. The ideal Otto cycle can be summarised into two different thermodynamic processes, an isentropic[1] process and an isochoric[2] process. The compression and expansion phase follows an isentropic process, and the adding of heat during combustion is adiabatic and isochoric.

With the adding of that the expansion of the cylinder gas at the gas exchange occurs instantly and follows an isentropic process, an ideal gas exchange process may be added to the Otto cycle. The ideal Otto cycle, with the additional gas exchange is shown in Figure 2.1.

As will be noted in later chapters, the residual gas (mass) fraction plays a vital role for the internal combustion engine. Thus, with the aid of an ideal Otto cycle with the additional ideal gas exchange process, one will find an expression for the residual gas fraction, x_{rg}, as,

$$x_{rg} = \frac{m_{rg}}{m_{tot}} = \frac{\frac{p_{EVC}V_{EVC}}{RT_{EVC}}}{\frac{p_{EVO}V_{EVO}}{RT_{EVO}}}, \qquad (2.1)$$

where the values of T_{EVO}, p_{EVO}, V_{EVO}, T_{EVC}, p_{EVC} and V_{EVC} will be derived at the event of the exhaust valve opening (EVO) and closing (EVC) respectively.

---

[1]i.e. with no heat transfer (i.e. adiabatic) and a reversible work the process will become isentropic.
[2]i.e. dV = 0.
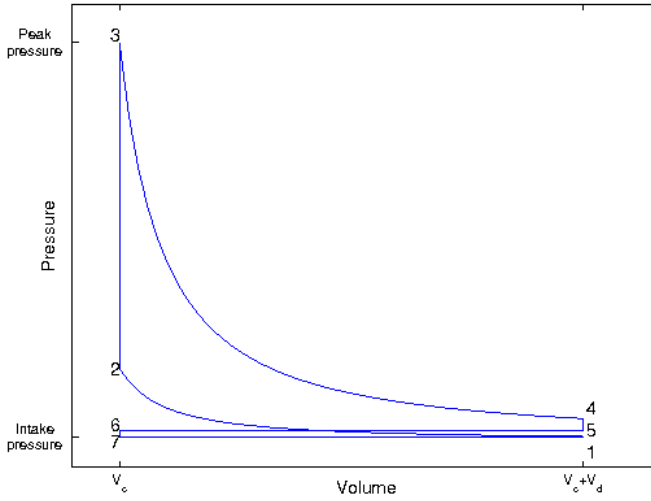
Figure 2.1. The ideal otto cycle with the additional gas exchange process. The numbers in the figure are refered to as: "1" being the start of compression, "2" the start of combustion, "3" the end of combustion and start of expansion, "4" the end of expansion, "5" burned gas expansion to the exhaust manifold pressure, "6" EVC and "7" IVO.

Thus, e.g. $p_{EVO} = p_{exp}$, is the cylinder pressure at the end of the isentropic expanison process, the same goes for $T_{EVO} = T_{exp}$ and $V_{EVO} = V_c + V_d$.

At EVC, the burned gas have undergone an isentropic expansion to the exhaust pressure, i.e.

$$p_{EVC} = p_{exh} = p_{EVO} \left(\frac{V_{tot}}{V_{EVC}} \right)^{\gamma}, \tag{2.2}$$

$$T_{EVC} = T_{exh} = T_{EVO} \left(\frac{p_{exh}}{p_{EVO}} \right)^{\frac{\gamma-1}{\gamma}} \text{ and} \tag{2.3}$$

$$V_{EVC} = V_c, \tag{2.4}$$

where $\gamma \equiv \frac{c_p}{c_v}$ and c_p and c_v are the specific heats[3]. With a reversible[4] process the specific heats can be expressed as follows,

$$c_p = \left(\frac{dh}{dT} \right)_p \text{ and} \tag{2.5}$$

$$c_v = \left(\frac{du}{dT} \right)_v. \tag{2.6}$$

---

[3]The energy needed for the increase of one degree of a unit mass

[4]A process where the path of the process is always infinitesimal close to its equilibrium conditions, is called a reversible process.

With the use of Equation 2.2– 2.3 in Equation 2.1, the following will hold,

$$x_{rg} = \frac{V_c}{V_{tot}} \left(\frac{T_{exh}}{T_{exp}}\right)^{\frac{1}{\gamma-1}} = \frac{1}{1+\frac{V_d}{V_c}} \left(\frac{T_{exh}}{T_{exp}}\right)^{\frac{1}{\gamma-1}}. \tag{2.7}$$

2.2   Heat Transfer

The transport of thermal energy occurs through three different types of heat transfer, *convection*, *conduction* and *radiation*.

Heat transfer to the cylinder wall in a spark ignited (SI) engine originates from heat transfer by convection. The conductive heat transfer that occurs between the cylinder wall and the coolant, is not of interest in this thesis. The heat transfer by radiation in a SI engine is insignificant in magnitude compared to the heat transfer by convection ([4]). Thus, it will be left aside.

Heat transfer to the cylinder wall is described by Newton´s law of cooling:

$$\dot{Q} = Ah(T - T_{Wall}), \tag{2.8}$$

where A is the contact area, h is the heat transfer coeffiecent, T_{wall} is the temperature of the cylinder wall, T is the temperature of the gas and $\dot{Q}$ is the heat transfer to the wall. The heat transfer coeffcent is an unknown parameter, it may, however, be estimated using the Nusselt, Reynolds and Prandtl numbers, as shown in [4]. For estimating the heat transfer coefficient, Equation 2.9 is used, which holds for a number of different flow geometries ([4]) (e.g. flow trough pipes).

$$Nu = C(Re)^m (Pr)^n \tag{2.9}$$

where Nu is the Nusselt number, Re is the Reynolds number, Pr is the Prandtl number, C, m and n are constants.

The Reynolds, Nusselt and Prandtl numbers are dimensionless quantities that are defined as,

$$Pr = \frac{\mu c_p}{k}, \tag{2.10}$$

$$Re = \frac{\rho v l}{\mu}, \tag{2.11}$$

$$Nu = \frac{hl}{k}, \tag{2.12}$$

where μ is viscosity, k thermal conductivety, c_p is the specific heat under constant pressure, ρ is density, v is gas velocity, l is the characteristic unit of length and h is the heat transfer coefficient.

2.2.1 Approximations

Annand, Hohenberg and Woschni, have all provided approximations for Equation 2.9. For this thesis Woschni´s approximation was used and is therefore presented further. The other two are presented in e.g. [4].

Woschni

Woschni found a good approximation to Equation 2.9 (see [11]) with,

$$Nu = 0.035 Re^m. \tag{2.13}$$

As noted in Equation 2.11, the Reynolds number depends on the velocity of the gas and Woschni further assumed that the gas velocity was proportional to the mean piston speed during the intake, compression and exhuast stroke, see [11]. During combustion and expansion, the gas velocity will increase due to the fact that the density changes. Hence, a term that is proportional to the pressure rise (at a fired cycle) compared to a motored cycle $(p - p_{motored})$, is added to the gas velocity. The derived gas velocity, for the gas exchange, compression and combustion is presented in Equation 2.14.

$$v = c_1 \bar{S}_p + c_2 \frac{V_d T_{IVC}}{p_{IVC} V_{IVC}} (p(\theta) - p_{motored}(\theta)), \tag{2.14}$$

where $\bar{S}_p$ is the mean piston speed (i.e. $\bar{S}_p = 2lN$, where l is the stroke and N is the engine speed) and θ is the crank angle. The values of the two constants c_1 and c_2, have been derived through experiments made by Woschni. The derived values are,

$$(c_1, c_2) = \begin{cases} (6.18, 0) & \text{during gas exchange,} \\ (2.28, 0) & \text{during compression,} \\ (2.28, 0.0034) & \text{during combustion and expansion.} \end{cases} \tag{2.15}$$

With the approximation of $\mu \approx T^{0.62}$ and $k \approx T^{0.75}$ from Woschni (1965) ([10]) and that the gas is ideal, in Equation 2.13, then the following will hold,

$$\frac{hB}{T^{0.75}} = 0.035 \left(\frac{\frac{p}{RT} vB}{T^{0.62}} \right)^m =$$

$$\underbrace{0.035 R^{-m}}_{c_3} p^m T^{-0.62m} V^m$$

$$\Longleftrightarrow$$

$$h = c_3 p^m T^{0.75 - 1.62m} B^{m-1} v^m \tag{2.16}$$

where the linear characterisc dimension has been taken as the cylinder bore (B) and Woschni ([11]) further suggested that the parameter m should be set to 0.8. (Note that, h is the heat transfer coefficient, not enthalpy.)

Chapter 3

Introduction to psPack

This chapter will give a brief introduction on the tool for simulation, important models and their built-in alternatives.

3.1   Modules

The simulation package, i.e. psPack, is built, or designed, to be modular. Therefore any adding, or removing, of a different implementation (i.e. a submodule) should be easy. Thus, there might be a vast number of implementations for any such module. The modules are combined into a model for simulation at an user friendly GUI[1]. A snapshot of the GUI is shown in Figure 3.1. For further information regarding the design of psPack, see [8]. The purpose of psPack is to give a better understanding on how the gas exchange process is affected by various valve settings.

3.2   Multi-Zone Model

A multi-zone model has several zones at which a fraction of the entire volume will be present.
The reason for a having a multi-zone, could be that of e.g. in a compression ignited (CI) engine, the charge is stratified, hence the fuel/air-ratio, ϕ, will differ throughout the cylinder. Also the calculation of emissions from a spark ignited (SI), or CI, engine requires an extensive temperature history. The temperature history, or trace, will provide neccessary data for deriving the different speciments after combustion. When this is not needed, a one-zone model is sufficient. The simulation package, psPack, has the implementation of both a two-zone model and a one-zone model.

---

[1]Graphical User Interface
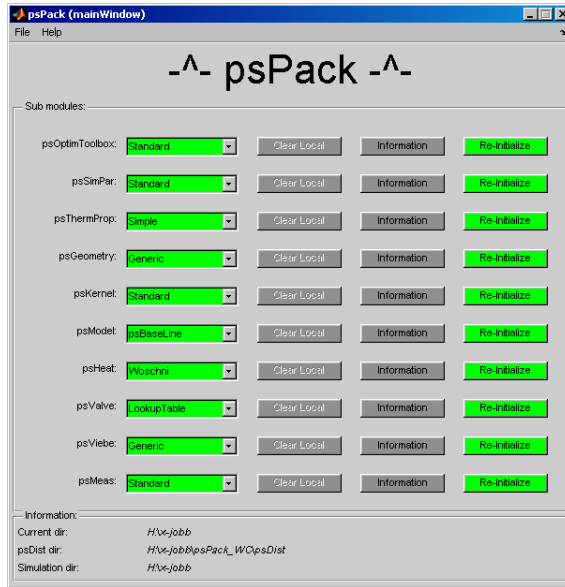
Figure 3.1. A snapshot of the psPack presentation GUI. Every submodule is represented to the left and has a dropbox to the right. The dropbox contains the available models for that submodule.

3.2.1   Two-Zone Model

During the gas exchange and combustion a two-zone model is used. This is from the fact that during combustion there will be a mass transfer from an unburned zone till a burned zone. During combustion the mass transfer will be according to the combustion efficiency, η_{comb}, of the total mass. The η_{comb} was set, with the help of data presented in [4], to 99%. The value of η_{comb} may be set arbitrary close to one, but it is essential that the simulation tolerances are changed accordingly, since it is unwise to set $\eta_{comb} < relTol$[2].

At the event of EVO, the last percent of unburned mass will burn. This in fact releases the energy instantaneously, but since the expansion pahse is finished, the added temperature will only be noticealbe in the exhaust manifold. In a case with backflow, this would however change the temperature of the residual gas. Which in turn would change the air charge for the next cycle. It is thought, however, that the relatively small effect that this has, is negligable.

3.2.2   One-zone model

Upon the event of IVC, the two-zones are instantly mixed into one zone. The mixing of the two-zones occurs under adiabatic[3] mixing conditions. Mixing is a free expansion process[4] where the internal energy does not change.

---

[2]$relTol$ is the global relative tolerance level for simulation

[3]i.e. $dQ = 0$.

[4]c.f Joules experiment.

3.3 Thermodynamic Properties

With the high pressure and temperature in an internal combustion engine, the number of molecules will change ($n = n(p, T)$). Also with $n(p, T)$, the molar mass will change, i.e. $M = M(T, p)$. Hence, the ideal gas state Equtaion 3.1, will not be valid. This is because of that the ideal gas constant, $R = \frac{\tilde{R}}{M(T,p)}$, will no longer be constant. Instead of Equation 3.1, Equation 3.2 will hold.

$$pV = n\tilde{R}T = mRT. \tag{3.1}$$

$$pV = mR(T, p, \phi, x_b)T. \tag{3.2}$$

To be able to use Equation 3.2, $R(T, p, \phi, x_b)$ must be derived. A program like the *Chemical Equilibrium Program Package (CHEPP)* ([3]), will provide the necessary thermodynamic properties, such as $h(T, p)$ for evaluating $R(T, p, \phi, x_b)$ in Equation 3.2. Other thermodynamic properties that may be needed are h, u, c_p, c_v, γ, R, $\frac{dR}{dT}$, $\frac{dR}{dp}$ and $\frac{dR}{d\phi}$.

3.3.1 Submodule of Thermodynamic Properties

Because of the properties mentioned above, there are, in psPack, several different implementations on how the gas should be treated. Since the calculation of thermodynamic properties is a potential time-consuming process, it is wise to use gas models that are accurate enough, within the region of interest. However, it is possible to call CHEPP, in every timestep to evaluate current thermodynamic properties. In the current implemenation of thermodynamic properties, the options range from a "Simple" gas composition, to a gas composition with air as its only content.

With the "Simple" gas composition, the gas is treated as an ideal gas in that sense that Equation 3.1, with the addition of that thermodynamic properties may change with ϕ and residual mass fraction, is valid. There are also assumptions made on $R(T, p, \phi, x_b)$[5] and it will fullfill the following, $\frac{dR}{dT} = \frac{dR}{dp} = 0$. It is also assumed that the specific heats, c_v and c_p, will be described by simple polynomials.

The somewhat lower temperature during the gas exchange compared to the temperature during combustion, will hold Equation 3.1 vaild. Thus, the assumptions made regarding R, c_v and c_p are valid, at least, throughout the gas exchange process.

There are also implementations of a "Simpler" and a "Simplest" variant of the gas composition.
With "Simpler", $R = R(\phi)$ i.e. the gas constant has some dependency on the fuel/air-ratio for the mixture. The specific heats are treated as constants.

With the third implementation, i.e. "Simplest", R, c_v and c_p will be regarded as constants.

---

[5]since ϕ and x_b are constants, they can be omitted. (x_b, is the burned mass transfer and is constant at each zone.)

There is also a fifth implementation, "Tables", that will let the user to specify an unique gas composition. The only request is that the user-defined gas will share the same structure as "Simple", "Simpler" etc.

Because of the excessively simplified models of "Simpler" and "Simplest", they were not chosen for the simulation. The selected implementation for simulation was "Simple".

3.4 Heat Transfer

The implementation of heat transfer is Woschni's heat transfer model. The choices left to be decided by the user are the two constants c_2 and c_3 in Equation 2.14 and Equation 2.16, respectively. The constant c_3 will indirectly change the parameter c_1.

Woschni´s model was first developed for the use of estimating the heat transfer in a CI engine. Thus, the suggested values on c_1 and c_2 in Equation 2.15 are derived from a measurments made with a CI engine.

As can be noted in Figure 12-10 and 12-16 in [4], the correlation at an instant during the cycle is quite poor. However, the estimation of heat transfer during a closed cycle is good (see e.g. [5] p.40). This was one of the main objectives with Woschni´s heat transfer model, (see Equation 1 in [11]). Therefore it is widely accepted and have been used in a large number of books, articles etc.

3.5 Burn Profile Model

With the use of a Vibe function (see [9]), the estimation on how much and fast the burned mass develops could be derived, c.f Equation 3.3, i.e. the mass transfer between the zones during combustion. For the derivative of the Vibe function w.r.t to crank angle, see Equation 3.4. The choices to be made with the Vibe function is to determine the different values of a, m and $\theta_{comb} = \theta_e - \theta_s$.

$$x_B = \eta_{comb}\left(1 - exp(-a\left(\frac{\theta - \theta_s}{\theta_e - \theta_s}\right)^{m+1})\right) \tag{3.3}$$

$$\frac{dx_B}{d\theta} = \eta_{com}\frac{a(m+1)}{\theta_e - \theta_s}\left(\frac{\theta - \theta_s}{\theta_e - \theta_s}\right)^m exp(-a\left(\frac{\theta - \theta_s}{\theta_e - \theta_s}\right)^{m+1}) \tag{3.4}$$

where θ is the crank angle, θ_s, θ_e are the crank angles for the start and end of combustion respectively and, a and m are design parameters. The combustion effeciency, η_{comb}, could be estimated with the help of data presented in Heywood (1988)(p.82 [4]). In [1], several different types of engines and operation points are presented togethter with a burn profile and the corrensponding values of a and m. The data could therefore serve as a first indication on the wanted values.

3.6   Engine Model

For the moment there is a pre-defined engine model in psPack which was also the one used for simulation. The model consist of control volumes[6], i.e. an intake pipe, and restrictions, i.e. a valve. Each volume is divided into three sections. Each sections will hold a plug, that will move in the direction of the flow, i.e. *upstreams* or *downstreams*.
The direction of a mass flow in an engine is to be considered as the flow of water in a river. Thus, *downstreams* (DS) would be the normal flow direction, i.e. from intake to exhaust. A flow *upstreams* (US) would therefore be in the opposite direction. A mixture that will flow downstreams, is considered to consist of either fresh or burned mixture. In the opposite flow direction, the mixture will be considered to be of burned mixture.
A restriction is treated as described in the system of equations 4.4.

3.6.1   Submodule for Engine Models

The geometry of pipes, intake manifold, cylinder volume, valve area and etc, can all explicitly be set by the user. However, there is a pre-defined engine[7] geometry that could be chosen. This option was also the one chosen for simulation.

3.7   Variable Valve Timing

One of the main objectives for psPack, was to create a simulation package, at which one could simulate the correct behaviour from a variable valve timing (VVT) engine during the gas exchange process.
Therefore, the user is left to fully control how the valve profile should look like, it is just a matter of defining it in the right way. However, there are valve profiles from a SAAB engine present, these could serve as an indication on how the profile should, or could, look like.

---

[6]A control volume is volume where user defined physics is said to hold.
[7]SAAB L850 engine

Chapter 4

Validation of Results Acquried From psPack

This chapter will serve as a small comparison between data from simulations to a set of measured data retrieved from Heywood (1988) [4]. It is wise, as stated in the introduction for this thesis, to have a copy of Heywood (1988) [4], at your side when reading this chapter.

4.1 Instantaneous Mass Flow of Exhaust Gas During Exhaust Phase

Due the lack of data from an instantaneous mass flow meter, figures and data provided in [4] will serve as the data for validation. In [4], Figure 6.20 is of interest, where engine measurements have been made for three different engine speeds. The same engine speeds as in Figure 6.20, were used for acquiring simulation data. The valve setting used during the measurement is not mentioned, therefore the standard, or normal, valve setting was used for the simulation.

The result from simulations are shown in Figure 4.1. (Note that Figure 4.1 is plotted against crank angle, not time.) The time when the mass flow is choked[1] at EV have been marked in the figure. By the comparison of Figure 4.1 and Figure 6.20 in [4], the two figures share the same general behaviour for the mass flow during the exhaust phase. However, the magnitude of mass flow during the blowdown, differs by a factor two, which is significant.

Because of the increased mass flow from simulation, an analysis based on the set of equations from a compressible and isentropic flow through a restriction, will be made.

---

[1]a choked (or critical) mass flow occurs when the velocity of the mass flow at the minimum area, throat, or restriction reaches the speed of sound

The section that follows, will hold an analysis on how a mass flow through a restriction can be derived from the set of equations in [2], yielded from such an analysis. The reader who is familiar with this, can skip forward to 4.1.2.
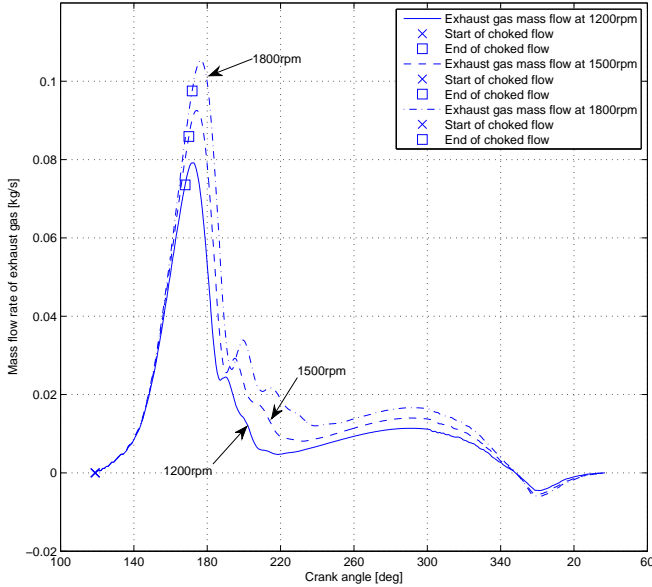
Figure 4.1. The mass flow of exhaust gas through the exhaust valve during the gas exchange process. As can be seen the exhaust mass flow is choked during a large part of the blowdown phase. The displacement phase is the result of the piston pushing gases out of the cylinder (some reflections are also noticeable).

4.1.1   Compressible and Isentropic Flow Through a Restriction

The same system of equations, yielded after an analysis made in [2] regarding a compressible and isentropic flow through a restriction, is presented in Equation 4.1.

$$
\begin{cases}
T_1 &= T_1^0 - \frac{c_1}{2c_p} \\
p_2^* &= \max\left\{p_2, p_1\left(\frac{T_1^0}{T_1}\frac{2}{\gamma+1}\right)^{\frac{\gamma}{\gamma-1}}\right\} \\
c_2 &= \sqrt{c_1^2 + 2c_pT_1\left(1 - \left(\frac{p_2^*}{p_1}\right)^{\frac{\gamma-1}{\gamma}}\right)} \\
T_2 &= T_1\frac{p_2^*}{p_1}^{\left(\frac{\gamma-1}{\gamma}\right)} \\
\rho_2 &= \frac{p_2^*}{R_2T_2} \\
\dot{m} &= \rho_2 A_{eff}c_2
\end{cases}
\tag{4.1}
$$

where subindex "1" and "2" indicate quantities before and after the restriction, respectively, c is the gas velocity.

By letting the gas before the restriction be at rest, i.e. $c_1 = 0$ (this could be seen as a relaxation of the dynamics) and the introduction of $\Pi = \frac{p_2^*}{p_1}$, the system of equations in 4.1 could be reduced to,

$$
\begin{cases}
p_2^* = \max\left\{p_2, p_1\left(\frac{2}{\gamma+1}\right)^{\frac{\gamma}{\gamma-1}}\right\} \\
c_2 = \sqrt{2c_pT_1\left(1 - \left(\frac{p_2^*}{p_1}\right)^{\frac{\gamma-1}{\gamma}}\right)} \\
T_2 = T_1\frac{p_2^*}{p_1}^{\left(\frac{\gamma-1}{\gamma}\right)} \\
\rho_2 = \frac{p_2^*}{R_2T_2} \\
\dot{m} = \rho_2 A_{eff}c_2.
\end{cases}
\Rightarrow
\begin{cases}
\Pi = \frac{p_2^*}{p_1} = \max\left\{\frac{p_2}{p_1}, \left(\frac{2}{\gamma+1}\right)^{\frac{\gamma}{\gamma-1}}\right\} \\
c_2 = \sqrt{2c_pT_1\left(1 - \Pi^{\frac{\gamma-1}{\gamma}}\right)} \\
T_2 = T_1\Pi^{\frac{\gamma-1}{\gamma}} \\
\rho_2 = \frac{p_2^*}{R_2T_2} \\
\dot{m} = A_{eff}\frac{p_2^*}{R_2T_2}\sqrt{2c_pT_1\left(1 - \Pi^{\frac{\gamma-1}{\gamma}}\right)}
\end{cases}
\tag{4.2}
$$

With the assumption that the gas is ideal and that the ideal gas constant R, is assumed to be same for the gas during the whole exhaust phase (in fact it has some dependency of temperature, see [2]), i.e. $R_1 = R_2 = R$.

The last equation in 4.2 can therefore be rewritten as,

$$
\begin{aligned}
\dot{m} &= A_{eff}\frac{p_1\Pi}{RT_1\Pi^{\frac{\gamma-1}{\gamma}}}\sqrt{2c_pT_1\left(1 - \Pi^{\frac{\gamma-1}{\gamma}}\right)} = \\
&\quad \{R > 0, \, T_1 \geq 0\} = \\
&\quad A_{eff}\frac{p_1}{\sqrt{RT_1}}\Pi^{\frac{1}{\gamma}}\sqrt{\frac{2c_pT_1}{RT_1}\left(1 - \Pi^{\frac{\gamma-1}{\gamma}}\right)} = \\
&\quad A_{eff}\frac{p_1}{\sqrt{RT_1}}\sqrt{\frac{2\gamma}{\gamma-1}\left(\Pi^{\frac{2}{\gamma}} - \Pi^{\frac{\gamma+1}{\gamma}}\right)} = \\
&\quad A_{eff}\frac{p_1}{\sqrt{RT_1}}\Psi(\Pi).
\end{aligned}
\tag{4.3}
$$

Hence, with $c_1 = 0$ in Equation 4.1, the following will yield,

$$
\begin{cases}
\Pi &= \max\left\{\frac{p_2}{p_1}, \left(\frac{2}{\gamma+1}\right)^{\frac{\gamma}{\gamma-1}}\right\} \\
\Psi(\Pi) &= \sqrt{\frac{2\gamma}{\gamma-1}\left(\Pi^{\frac{2}{\gamma}} - \Pi^{\frac{\gamma+1}{\gamma}}\right)} \\
\dot{m} &= A_{eff}\frac{p_1}{\sqrt{RT_1}}\Psi(\Pi)
\end{cases}
\tag{4.4}
$$

Therefore, the last equation in the system of equations 4.4, will describe the mass flow through EV during both the blowdown and displacement phase. When the mass flow is choked, i.e. $\Pi = \left(\frac{2}{\gamma+1}^{\frac{\gamma}{\gamma-1}}\right) = Const$, the mass flow will only depend on the valve lift (i.e. A_{eff}) and gas properties, such as pressure and temperature upstreams of the restriction. Note that $\frac{p}{RT}$ is the density of the flowing gas.

4.1.2   Discussion

The main difference between Figure 4.1 and Figure 6.20, occurs during the blowdown phase, i.e. the part of the exhaust phase that mainly consists of a mass flow that is choked.

From Equation 4.4, Equation 4.5 can be retrieved. Thus with a choked flow the mass flow will solidly depend on the closed cycle[2] setup (i.e. gas properties such as temperature and pressure) and the valve profile (i.e. the valve lift and the effective flow area),

$$\dot{m} = A_{eff}\rho_1\sqrt{RT_1}\Psi(\Pi). \tag{4.5}$$

Closed Cycle Setup

The differences in density and temperature between simulation data and measured data, can reside from the fact that both the compression ratio, r_c and ϕ, differs. The measured data, has been run at a fuel-rich mixture, $\phi = 1.2$ and at a $r_c = 7$. The simulated data has a mixture at $\phi = 1$ and $r_c = 9.5$.

With a higher compression, both the density and temperature of the gas, during the entire cycle, will be higher.

With a greater content of air, i.e. a leaner air/fuel-mixture, the air/fuel-mixture will be combusted to a greater extent compared to a fuel-rich mixture, i.e. the temperature will be higher for a lean-mixture. With a fuel-rich mixture used at the measured data, the fuel vaporization process will lower the temperature for the air/fuel-mixture. Thus, this will further increase the gap in temperature between the simulated and measured data.

Valve Profile/Settings

The valve profile will have a considerable impact on both the magnitude and how fast the maximum mass flow can be obtained. This is probably the reason as to why the blowdown phase occurs more rapidly (i.e. at less crank angles) in Figure 4.1 compared to Figure 6.20 in [4].

In Figure 6.20 it can be noted that the mass flow corresponding from the highest engine speed, has only a small dip in mass flow at the transition between the blowdown and displacement phase.

---

[2]i.e. both IV and EV are closed

This, however, can not be noted at either of the engine speeds for the simulated data (c.f Figure 4.1). The reason for this is probably that the area for the exhaust valve used in [4], is smaller compared to the one used at simulation. Since a smaller valve area will be a greater restriction, the masss flow must therefore be higher during the entire exhaust phase. Hence, the valve area, used for simulation, is greater than the one used in [4].

The impact of a greater or lesser exhaust valve area, some 30%, are shown in Figure 4.2. It can be noticed that the decreased valve area will restrict the mass flow during the blow-down phase, i.e. there will not be a sharp decline of mass flow at the transition between the blowdown and displacement phase.

During the displacement phase both Figure 6.20 in [4] and Figure 4.1 share the same magnitude and behaviour, i.e. the two engines are comparable in engine volume. Also, the isentropic and compressible mass flow at the displacement phase is very similiar to that of Figure 6.20 in [4].
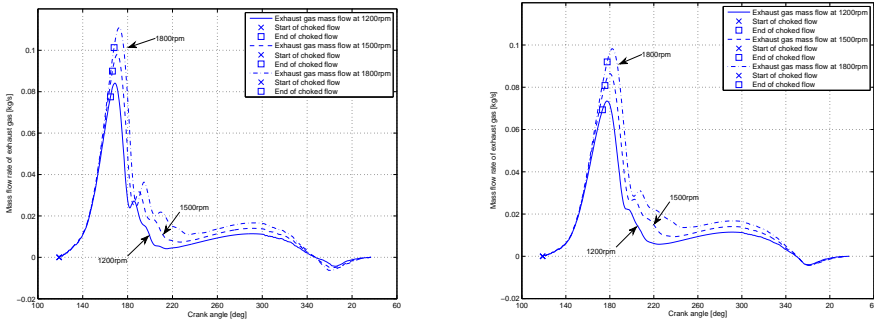
(a) Exhaust gas mass flow through a 30% greater exhaust valve area.

(b) Exhaust gas mass flow through a 30% lesser exhaust valve area.

Figure 4.2. The mass flow of exhaust gas through the exhaust valve during the gas exchange process, with the effect of a change in area for the exhaust valve area. It can be noted that the smaller valve area will restrict the mass flow at the blowdown, thus there will not be a sharp decline in mass flow at the transition between the blowdown and displacement phase.

Choked Mass Flow

By examining Figure 6.20 in [4], the blowdown phase (i.e. $M > 1$ in Figure 6.20 [4]) appears to occur during a greater number of crank angles, compared to Figure 4.1. The reason for this could be that the pressure quotioent between the in-cylinder and the exhaust manifold pressure, increases too quickly. Thus, the number of crank angles with a choked mass flow, will decrease.

It can also be noted in Figure 4.1, that the number of crank angles at choked flow, will increase with engine speed. This is from the fact that the blowdown will have less time, i.e. a greater number of crank revolutions occurs at less time.

4.1.3 Conclusion

With differences in closed cycle setup (i.e. the density and the temperature of the mixture) and, probably, valve settings (i.e. valve area/lift and etcetera), the difference in magnitude for the exhaust gas mass flow, is likely to be caused by these two factors, i.e. a different valve setting and setup for the closed cycle (c.f Equation 4.5).

4.2 Volumetric Efficiency

A small comparison was made for the volumetric effiency between the simulation data and Figure 6.11 in [4]. In Figure 6.11 in [4], both the valve overlap and valve duration have been altered. The valve settings where changed to meet the same valve settings as presented in Heywood. The valve settings used for validation are presented in Table 4.1.

Valve timing	10	0	19	10	30	20
	15	50	45	60	70	60
p_{IM}	Wide Open Throttle					

Table 4.1. The different valve settings used as the comparison between Figure 6.11 in Heywood and simulation data retreived from psPack. The row describing the different valve timing should be treated as the crank angles where: IVO (before TDC) upper left, IVC (after BDC) lower left, EVO (before BDC) lower right and EVC (after TDC) upper right.

The definition of η_{vol} is presented in Equation 4.6.

$$\eta_{vol} = \frac{m_{air}}{\rho_a V_d},$$ (4.6)

where ρ_a is set as the density for ambient air.

In Figure 4.3, the volumetric efficiency, η_{vol} has been plotted against engine speed. This figure should be compared to Figure 6.11 in [4]. The data gathered from simulations are of wider range of engine speeds than those presented in [4]. This is because of the vast effect that a combination of intake pipe lengths and engine speeds, i.e. gas velocities, has on the volumetric efficiency. Thus for yielding the same behaviour as in Heywood the maximum engine speed was increased to compensate for the, probably, different length of intake pipes.

From Figure 4.3, it is evident that the valve timing and duration plays a vital role for η_{vol}. The valve setup with the smallest valve overlap and duration, yield a decreasing effect on η_{vol} as the engine speed increases.

The time when IV is open is decreased at higher engine speed, hence with a small overlap and duration there will not be enough air inducted during the intake phase to sustain the higher η_{vol}. At low engine speeds this valve timing yield the highest η_{vol} and the reason for this is partly because of its small valve overlap.
The small valve overlap will minimise the backflow through IV and therefore minimise the amount of residual gas.

The other part is that, at a low engine speed, i.e. at low mass flows, the air charge flowing into the cylinder has a small inertia, i.e. the flow direction for the gas, or air charge, can be affected by the piston (with IV still opened) as it starts the compression. Thus, it is not wise to have IV open long after BDC at low engine speed, since the motion of the piston will push air charge through IV and thus reducing the volumetric efficiency. This effect can be avoided with an earlier closing of the intake valve, which is being done at this valve setting and therefore minimising the effect of fresh mixture being pushed out of the cylinder.

The backflow effect at low engine speeds is evident for the two other valve setups. They both suffer from this, thus yielding a lower η_{vol}. But as engine speed increases, they will give a higher η_{vol}.

The valve duration is also an important part of η_{vol}. With less valve duration, the raming, or trapping, efficiency will decrease, thus decreasing n_{vol}. Ram effects occur at the period from TDC to IVC. This is because of the inertia of the gas, thus it will take time for the gas to change its direction, hence the amount air that can be inducted during the intake phase will increase. This effect is clearly noticable for the low valve duration setup. When gas velocities, i.e. engine speed, increase, this effect will not be apperant for the low valve duration. Thus decreasing η_{vol} at high engine speeds.

However, there are some divergencies with the Figure 6.11 and Figure 4.3. The valve setting with IV: 30/70 EV:60/20, does not yield the same behaviour for η_{vol} as the data in Figure 6.11 ([4]). In Figure 6.11 the trend is obvious, an increase in engine speed will increase η_{vol}. This, however, is not that obvious in Figure 4.3 at the same valve setting. The reason for this is most likely that the intake pipes in [4] are more tuned to fit this valve timing and thus yielding a higher η_{vol}. Since the information regarding the size of the intake pipes is not presented, the intake pipes used for simulation were not altered. Thus, the formation of peaks will differ since, most likely, the size of the intake pipes differs.

The valve setting IV: 19/45 EV: 60/10, yields the same sort of behaviour as in Figure 6.11 ([4]). The peak in η_{vol}, is not as evident in Figure 4.3 compared to Figure 6.11, but the overall shape is the same.

However, the overall η_{vol} is somewhat lower for the simulation data than with the measured data. This could be explained by the same reason that were discussed in section 4.1 Which is that the gas temperature is higher at simulation than with measured data. With an increased temperature the η_{vol} will decrease (the density increases). But in total the two figures share the same type of results.
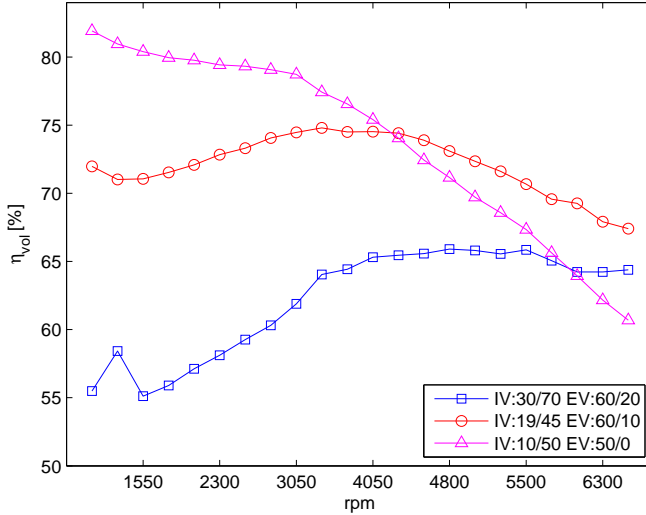
Figure 4.3. Volumetric efficiency plotted against different engine speeds. The valve timings are set as presented in Table 4.1. The effect of differet valve duration and timing, on η_{vol}, is noticeable as the engine speed increases.

Chapter 5

Simulation Setup

This chapter presents the selected operation points, why they have been selected and how the operation points have been set in psPack. There will also be a presentation of some interesting quantities that were derived from the simulation data.

5.1   Operation Point Setup

The different simulation setups involve three different valve settings, intake pressures and engine speeds. They have been combined to form a total of 27 different operation points.

(As will be noted in Chapter 6, not all of these operation points provided results that were correct. Thus, some of the combinations have been removed.)

Valve timing	5	24	26	36	55	74
	77	73	56	61	27	23
Engine speed	1600 RPM		2800 RPM		4000 RPM	
p_{IM}	0.5bar		1bar		1.3bar	

Table 5.1. The different operation points used during simulation. The combination of them will generate 27 different operation points. The row describing the different valve timing should be treated as the crank angles where: IVO (before TDC) upper left, IVC (after BDC) lower left, EVO (before BDC) lower right and EVC (after TDC) upper right.

5.1.1   Intake Manifold Pressure

Three different engine loads where used during simulation. Because of the direct correlation between engine load and intake pressure, the intake pressure could therefore be treated as the engine load.

Since the intake manifold pressure can not be set directly in psPack, the data from an engine map were utilized.

The data was used to determine both the pressure before the throttle and the effective throttle area. The following procedure was used:

From [6] it is clear that the airflow into the cylinder can be described as:

$$\dot{m}_{air,cyl} = \eta_{vol} \frac{NV_D p_{IM}}{n_r R_{IM} T_{IM}}, \tag{5.1}$$

where η_{vol} is the volumetric effiency and n_r is the number of crank revolutions for every power (expansion) stroke per revolution, i.e for a four-stroke engine $n_r = 2$. The airflow through the throttle plate can be derived with Equation 4.3

$$\dot{m}_{air,thr} = \frac{p_{US}}{\sqrt{R_{US} T_{US}}} A_{thr} C_D \Psi(p_r), \tag{5.2}$$

$$p_r = \frac{p_{DS}}{p_{US}} \tag{5.3}$$

where $p_{DS} = p_{IM}$, $p_{US} = p_{bef,thr}$, C_D discharge coefficient and $A_{thr} C_D = A_{eff,thr}$. Ψ is the pressure ratio function from Equation 4.4. At steady state, Equation 5.1 and 5.2 are equal. Hence,

$$\eta_{vol} \frac{NV_D p_{IM}}{n_r R_{IM} T_{IM}} = \frac{p_{bef,thr}}{\sqrt{R_{amb} T_{amb}}} A_{eff,thr} \Psi(p_r).$$

$$\Longleftrightarrow$$

$$A_{eff,thr} = \frac{\eta_{vol} V_D N p_{IM} \sqrt{R_{amb} T_{amb}}}{n_r R_{IM} T_{IM} \Psi(p_r) p_{bef,thr}}, \tag{5.4}$$

where $\eta_{vol} \approx 0.9$, $n_r = 2$ and $p_{bef,thr}$ was determined using data from the engine map (at the desired intake pressure and engine speed).

5.1.2 Engine Speed

The chosen engine speeds were selected in conjunction with the available intake manifold pressures from a provided engine map. With this in mind the chosen engine speeds were 1600, 2800 and 4000 RPM.

5.1.3 Valve Timing

The different valve timings used during simulation have been introduced in Table 5.1. As can be noted in Table 5.1, the valve duration does not vary between the different valve settings. In Chapter 3, the alternatives for setting the valve profiles in psPack were discussed. Since the same valve duration will be used, the same valve lift profiles may be used. Thus, the information needed by psPack, is the crank angle at which the valve profile is at its Maximum Open Position (MOP).

The MOP occurs roughly halfway through the valve duration. The three different valve timings that were used the notation presented as Table 5.2. The different valve profiles,

Valve timing	5	24	26	36	55	74
	77	73	56	61	27	23
Corrensponding MOP, IV/EV	485/240		464/252		435/290	

Table 5.2. Valve timing represendaded as the crank angle where the Maximum Open Position (MOP) occurs. The presentation of the table is the same as Table 4.1.

or timings, can be seen in Figure 5.1. Note that Figure 5.1, states the fraction of opening area and not valve lift. Even if the lift profile has a unique MOP the area fraction profile may be flat. The differen valve settings, were chosen from the fact that the maximum and minimum valve overlap are dead points for the phasing and the third one was chosen as it offers a standard valve overlap.
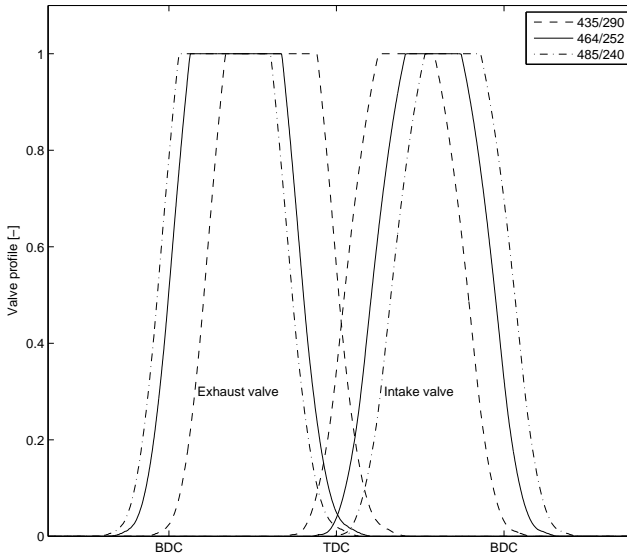
Figure 5.1. The three different valve profiles, with the corrensponding MOP values as presented in Table 5.2. The figure states the fraction of valve opening area, not valve lift, thus the curve will be flat when the valve lift reaches a certain length. That is, even though the valve lift increases, the fraction of opening area will not. The limits are elsewhere.

The change of valve setting was made before each simulation. Hence, only stationary conditions were simulated. On the other hand, at the transient there are some interesting phenomenons occuring. The cam phasing shift has a speed of 100 deg/s (CA revolutions), and any effect on the valve duration will have a vast impact. A maximum relative difference of 80% in mass flow and 20% in residual gas has been noted by Öberg et. al [7], during the transient.

5.2   Parameter Setup

Along with the different operation points, the value for several design parameters were also varied. They were changed $\pm$ 5% from their nominal value. The parameters that had their values altered are given in Table 5.3.

Parameter	Nominal value	Parameter	Nominal value
V_c	58.8 cm^3	$Duration$	60 ATDC
$Phasing$	10 ATDC	$L_{P,EM}$	10.0cm
$A_{P,EM}$	12.8cm^2	$L_{C,EM}$	5.00cm
$A_{C,EM}$	25.0cm^2	$L_{P,IM}$	10.0cm
$A_{P,IM}$	15.0cm^2	$L_{C,IM}$	10.0cm
$A_{C,IM}$	100cm^2	A_{IV}	16.0cm^2
A_{EV}	12.0cm^2	Fr_{EM}	250
Fr_{IM}	250	T_{Walll}	470K

Table 5.3. The parameters that have been altered during simulation.

(The nominal values have been taken from a SAAB L850 engine.) Most of the parameters are selfexplanatory, therefore some of them do not need any further presentation. The parameter $Duration$ is not the valve duration, but instead it is the burn duration for the air/fuel mixture during combustion.
The parameter $Phasing$ set at which CA 50% of the total mass should have burned.
The parameters Fr_{EM} and Fr_{IM}, sets the pipe friction in the exhaust and intake manifold respectively.

5.3   Number of Simulations

With the use of 16 different parameters and 27 operation points, the number of simulations that provided useful data[1] were 792. From the fact that each simulation took some 3-4 hours of computing, this thesis would never have ended in any reasonable time. The simulations were therefore performed in a parallel manner.

5.4   Extracting Useful Data From Simulations

5.4.1   Average Exhaust Temperature

For measuring the thermal energy blown out of the cylinder during the blowdown and exhaust stroke an average exhaust temperature has been computed.

---

[1]this will be noted in chapter 6

Because of the substantially varying mass flow through EV during the exhaust stroke (c.f Figure 5.2), a time-averaged exhaust temperature will not correspond well to the average energy in the exhaust gas.
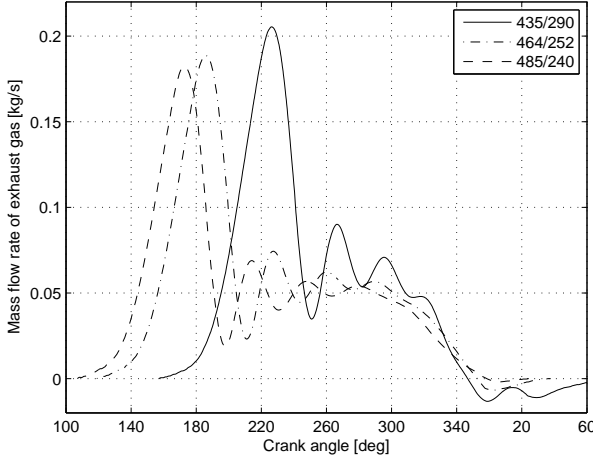
Figure 5.2. The mass flow out of EV during the blowdown (i.e from EVO to BDC) and displacement phase (i.e BDC to EVC), i.e the exhaust phase, for the three different valve settings used during simulation. Since the valve duration was not subject to change, the exhaust phase could be seen to occur at a later CA as the valve overlap increase.

For a better indicator on the thermal energy in the exhaust gas, an enthalpy-averaged temperature has been used, (see [4] p.234) (note that letter cased thermodynamic quantities are mass specific quantities):

$$\tilde{h} = \frac{\int_I \dot{m}_{EV} h \, d\theta}{\int_I \dot{m}_{EV} \, d\theta} \text{ where } I = \{\forall \theta : \theta_{EVO} \leq \theta \leq \theta_{EVC}\}. \tag{5.5}$$

Since

$$c_p = \left(\frac{dq}{dT}\right)_p = \left(\frac{dh - V \, dp}{dT}\right)_p = \left(\frac{dh}{dT}\right)_p, \tag{5.6}$$

$$dh = \tilde{h} - h_{calc}, \tag{5.7}$$

where both h_{calc} and c_p have been evaluated using *psThermProp* (i.e *CHEPP*). Therefore

$$dT = T_{wanted} - T_{guess} \iff T_{wanted} = dT + T_{guess}, \tag{5.8}$$

where T_{guess} is a first guess of the temperature at the desired $\tilde{h}$. T_{guess} is therefore the start temperature for the iteration towards the wanted temperature, T_{wanted}.
A simple Newton-method has been used for that iteration:

1. Set δ and T_{guess}.

2. Evaluate c_p and h_{calc}, with *psThermProp* at T_{guess}.

3. Calculate $\Delta T = \frac{\tilde{h} - h_{calc}}{c_p}$.

4. Thereafter $T_{guess} = \Delta T + T_{guess}$

5. If $|T_{guess}\delta| < |\Delta T|$ repeat the steps 1-5

6. Otherwise $T_{wanted} = T_{guess}$

Followed by step 6, T_{wanted} is the desired enthalpy-averaged exhaust temperature, $T_{Av,Exh}$.

5.4.2   Mixing Temperature

Upon the event of IVC the two zones are instantly mixed into one zone. The mixing temperature, T_{Com}, that have been used for analysis and discussion, relies on the following:

Assume that the fresh mixture has a constant $c_{v,fm}$ (specific heat for fresh mixture) and T_{fm}, the same should hold for the residual gas. The internal energy, u, could be expressed as,

$$u = c_v T, \quad \text{since} \quad \left(\frac{du}{dT}\right)_v = c_v.$$

Therefore, the conservation of energy will yield:

$$U_{after} = U_{before} \Rightarrow$$

$$(m_{rg}c_{v,rg} + m_{fm}c_{fm})T_{Com} = m_{fm}c_{v,fm}T_{fm} + m_{rg}c_{v,rg}T_{rg}$$

$$\text{and } m_{tot}x_{rg} = (m_{rg} + m_{fm})x_{rg} = m_{rg} \Rightarrow$$

$$\big((1 - x_{rg})c_{fm} + x_{rg}c_{v,rg}\big)T_{Com} = (1 - x_{rg})c_{v,fm}T_{fm} + x_{rg}c_{v,rg}T_{rg}$$

$$\Longleftrightarrow$$

$$T_{Com} = \frac{(1 - x_{rg})c_{v,fm}T_{fm} + x_{rg}c_{v,rg}T_{rg}}{\big((1 - x_{rg})c_{fm} + x_{rg}c_{v,rg}\big)}. \tag{5.9}$$

Hence, with the conservation of energy T_{Com} will be the mixing temperature.

5.4.3   Backflow

The backflow through a valve may be derived as:

$$m_{bf,i} = \int_I \dot{m}_{EV}\,dt, \text{ where } I = \{\forall t : u_i(t)^2 > 0\} \text{ and } i = \{EV, IV\}.$$

---

[2]u_i is the control signal for valve i. $u_i \in \mathbb{R}\{0, 1\}$

Chapter 6

Most Significant Model Paramters

This chapter will present the simulation results, along with a discussion of the results.

6.1 Simulation Results

The simulation results were put together in to a number of different tables. Each table represents one operation point setup, e.g 2800 RPM. Therefore some information on how to read tables will be needed.

6.1.1 Representation Of Columns

Each table is divided into seven different columns;

"Quantity", the considered quantity,

"Parameter", the name of the considered parameter on that row,

"Quotient", the relative difference between the 105%-value and the 95%-value. For PPP the value in this column will be an absolut difference between the 105%-value and the 95%-value. (It is more interesting to see how much PPP differ in actual degrees.). If "Quotient"$\leq 10^{-3}$, the result from that simulation will be considered insignificant. The "Quotient"-value will express the level of significance between the parameter and quantity.

Columns 4–6 contributes information regarding the operation point that this row concerns,

Lastly the column named "Ind."(short for "Indication") provides information regarding how the parameter and the quantity correlates. (i.e, an upward (downward) pointing arrow signifies that an increase in the paramter value will increase (decrease) the quantity, i.e the correlation is positive (negative).)

6.1.2 Quantities Used for Analysis

The quantities used for analysis were Peak Pressure (PP), Peak Pressure Position (PPP), $T_{Av,Exh}$ (i.e. the enthalpy-averaged exhaust temperature derived in Chapter 5), the residual gas mass fraction (x_{rg}) and the air mass flow into the cylinder ($\dot{m}_{air}$). These quantities were chosen because of two reasons.

Firstly, the values for the chosen quantities are the result of the gas exchange process, i.e. if a parameter affects any of these five quantities then it can be concluded that it have had an effect on the gas exchange process. For example, if a change in a parameter value will yield less fresh mixture to be inducted during the gas exchange process, then it will be first noticeable at $\dot{m}_{air}$ and x_{rg} (since the amount of residual gas will increase) and thereafter in PP, PPP and the exhaust temperature since they reflect the energy that is released during combustion, thus these quantities will reflect a change in air charge during the gas exchange process.

Secondly, PP, PPP and $\dot{m}_{air}$ can be measured (directly) at an experiment and can therefore easily be used to verify simulation results. Even though both x_{rg} and $T_{Av,Exh}$ can not be measured directly at an experiment, they can however be derived from experimental data and therefore also verify simulation results.

6.1.3 Organizing the Tables

As noted in 5.3, the number of simulations were vast. Therefore, the parameters that provided the top five greatest relative differences for the given quantity was used to form a "Maximum relative difference"-table. Such a table will only serve as a guide line on the correlation for that parameter and quantity. In some cases the information provided by this table, i.e the guide line, were not enough for analysing the correct behaviour from that parameter and an extended version of that table were therefore created. The extended table provides information regarding the parameter and quantity in that specific operation point setup. (The extended tables are presented in Appendix B.) An operation point setup consits of either one engine speed, valve setting or intake manifold pressure. E.g. a table representing the simulation results from an engine speed at 1600 RPM, will have all of the available valve settings and intake manifold pressures, freely variated.

The different operation point setups include the three different engine speeds, valve settings and intake manifold pressures. Each one of these operation point setups, has a "Maximum relative difference"-table. Thus, there is a total of nine different "Maximum relative difference"-tables.

6.1.4 Sifting Through The Operation Points

Because of the assumptions made with psPack regarding gas flows in an engine, c.f 3.6, a cross flow of fresh mixture through the cylinder can provide incorrect simulation data (compared to physical data). A cross flow occurs at high intake pressures and great valve overlaps.

All, or some, of the exhaust gases in the cylinder will be pushed out by the fresh mixture. Eventually the fresh mixture will also find its way into the exhaust pipe. (This can only take place during the time when both the IV and EV are open at the same time, i.e the valve overlap period).

Because of the reflections from gases in the exhaust pipe when e.g. hitting the end of the exhaust pipe, or by being reflected by some other cylinders blowdown, will cause a backflow through EV into the cylinder. This is evident as EV is about to close. The backflow through EV will then, according to psPack, consist of exhaust gas, when it in fact could be fresh mixture. Thus, this could produce false data.

Results from one of these operation points could be witnessed in Figure 6.1.
At the event of IVO, the burned gas volume, V_{bg}, will almost entirely be diminished. This is because of the high intake pressure (as seen in Figure 6.1(b)) with fresh mixture pushing the burned gas out of the cylinder. During the backflow through EV, V_{bg} will yet again become a non-zero volume and it will increase as the backflow through EV increases (c.f Figure 6.1(b)).

This can only occur with fresh mixture first entering the exhaust pipe and then during the backflow through EV flow back into the cylinder, being recorded as exhaust gas when its in fact is fresh mixture.

In Figure 6.1(c) the valve profiles of EV and IV is shown. Figure 6.1 is plotted with unchanged parameter values (i.e this will hold for every parameter). The operation points that are affected by this are:
the valve setting IV/EV 435/290, the intake pressure at 1.3bar and all of the engine speeds. Therefore none of these three operation points will be investigated. (Note that this does not happen when residual gas expands into the intake pipe/manifold. Therefore it is not a problem with backflow through IV.)

6.2   Simulation Results From 1600 RPM

This section will deal with the results from simulations regarding the different operation points at 1600rpm. The operation point with the greatest overlap (IV/EV 435/290) is clearly the most frequent operation point in Table 6.1.

The reason for this could be seen in Figure 6.2, where the amount of residual gas, x_{rg} is readily effected by the valve setting. This is from the fact that with an increase of valve overlap, the backflow through IV is increased[1]. There will also, at EVC, be a backflow through EV. This will occur because of the difference in pressure between the intake pipe/manifold and the exhaust pipe/manifold. Any effect, e.g. a reflection, that will increase the pressure behind EV, will further enhance this backflow.

---

[1]at intake pressure less than that of the cylinder
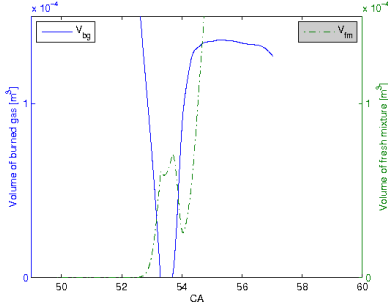
(a) V_{bg} and V_{fm} plotted against CA, during the gas exchange process.
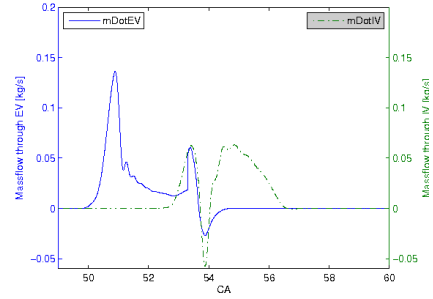
(b) $\dot{m}_{IV}$ and $\dot{m}_{EV}$ plotted against CA, during the gas exchange process. The increase of $\dot{m}_{EV}$ at IVO, is comparable to that of $\dot{m}_{IV}$.
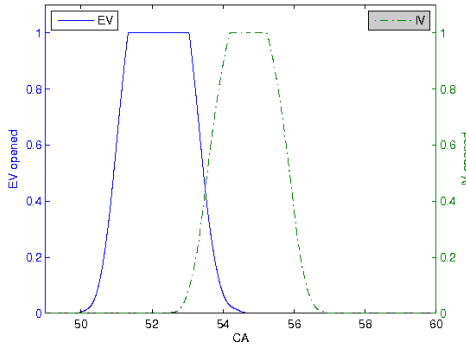
(c) u_{IV} and u_{EV}, i.e the valve profiles for IV and EV, plotted against CA. ("1" represents a fully opened valve and thus "0" represent a closed valve.)

Figure 6.1. V_{fm}, V_{bg}, $\dot{m}_{EV}$, $\dot{m}_{IV}$, u_{IV} and u_{EV} plotted against CA at the operation point described in section 6.1.4. In Figure 6.1(a), V_{bg} could be seen, during the exhaust phase, to decrease. At IVC, V_{bg} is almost fully diminished by the high intake pressure. The backflow through EV, at the closing of EV, is recorded as exhaust gas. This could be seen in Figure 6.1(a), where V_{bg} increases during the backflow.

Quantity	Parameter	Quotient	RPM	p_{IM}	IV/EV	Ind.
PP	V_c	0.0888	1600	0.5	435/290	↘
PP	$Phasing$	0.0239	1600	1	435/290	↘
PP	$Duration$	0.0149	1600	1.3	485/240	↘
PP	A_{EV}	0.0100	1600	1	435/290	↘
PP	T_{Wall}	0.0099	1600	1.3	485/240	↘
PPP	V_c	0.7656	1600	0.5	435/290	↗
PPP	$Phasing$	0.7339	1600	1.3	485/240	↗
PPP	$Duration$	0.6551	1600	0.5	435/290	↘
PPP	A_{EV}	0.1019	1600	0.5	435/290	↘
PPP	T_{Wall}	0.0818	1600	0.5	435/290	↘
$T_{Av,Exh}$	V_c	0.0243	1600	1	435/290	↗
$T_{Av,Exh}$	T_{Wall}	0.0168	1600	0.5	435/290	↗
$T_{Av,Exh}$	$Phasing$	0.0055	1600	0.5	485/240	↗
$T_{Av,Exh}$	A_{EV}	0.0045	1600	0.5	435/290	↘
$T_{Av,Exh}$	$Duration$	0.0021	1600	1.3	485/240	↗
x_{rg}	V_c	0.0852	1600	1.3	485/240	↗
x_{rg}	A_{EV}	0.0654	1600	1	435/290	↗
x_{rg}	T_{Wall}	0.0213	1600	1	435/290	↘
x_{rg}	A_{IV}	0.0150	1600	0.5	435/290	↗
x_{rg}	$A_{p,EM}$	0.0124	1600	1.3	464/252	↘
$\dot{m}_{air}$	A_{EV}	0.0226	1600	0.5	435/290	↘
$\dot{m}_{air}$	T_{Wall}	0.0134	1600	1.3	485/240	↘
$\dot{m}_{air}$	V_c	0.0071	1600	0.5	435/290	↘
$\dot{m}_{air}$	$A_{C,IM}$	0.0067	1600	0.5	435/290	↗
$\dot{m}_{air}$	$L_{C,IM}$	0.0067	1600	0.5	435/290	↗

Table 6.1. The five most significant parameters for PP, PPP, $T_{Av,exh}$, x_{rg} and $\dot{m}_{air}$, while low RPM are being considered.

The valve overlap will also affect the intake manifold pressure. This is from the fact that the valve duration is held constant throughout the different valve settings (c.f Table 5.1). Thus, the different valve settings will only adjust at which CA a valve should open or close (i.e the valve overlap will only be affected).

With an intake valve that opens earlier (and the exhaust valve still opened), the exhaust gas will expand into the intake pipe (i.e a backflow through IV). With the valve duration left unchanged, IV will stay opened for the same number of crank angles as with any other valve setting. Thus, the number of crank angles when there is only air flowing into the cylinder is shortened. Therefore, with the increased flow of exhaust gas into the intake manifold and the decreased flow of air mass flow into the cylinder[2], the intake manifold pressure will increase.

---

[2]i.e the residaul gas mass fraction will increase.

With a later (in CA) opening of IV (and EVC occurs earlier), the air mass flow will not be that affected, compared to the case described in the paragraph above, by the flow of exhaust gas into the intake manifold.

Thus, because of the mentioned above, there will be differences in magnitude for the different valve settings and intake manifold pressures.
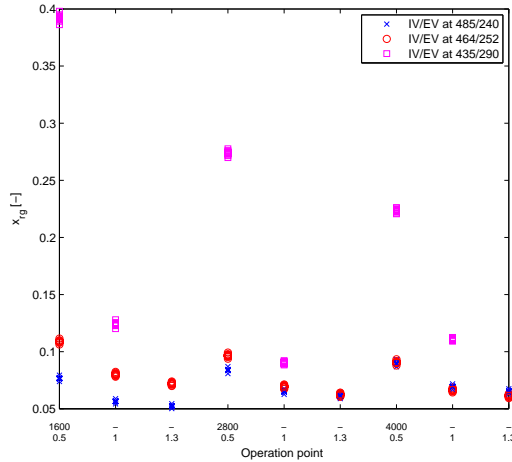
Figure 6.2. The residual gas mass fraction, x_{rg}, plotted for the different operation points, where the three different valve settings have been marked as shown in the figure. With a change of valve overlap, the amount of residual gas is vastly affected. (The horizontal axis has two different rows, the first row marks the RPM and the second row marks the valve setting. The '-' sign is used if the RPM does not change from the previous operation point.)

The second most common operation point is the low intake pressure (or low load). The reason for this is the same as stated above. The low intake pressure will further enhance the backflow effect. The amount of residual gas will therefore increase. Figure 6.3, show the correlation between a low intake pressure and a high content of residual gas.
One intresting note is that, parameters from the exhaust side are more significant than those on the intake side, as can be seen in Table 6.1. This could be from the fact that if a parameter effects the amount of residual gas, e.g. enhancing the effect of a backflow, then it will produce significant results. This is explained by the fact that parameters that affects the residual gas mass fraction, or temperature, has a significant effect on the air charge.

6.2.1 Ideal Otto cycle

Most of the analysis made in the following sections relies upon an ideal Otto cycle[3], as presented in Chapter 2. With the ideal Otto cycle, iterations on how pressures and

---

[3]when spoken of the ideal Otto cycle (in this thesis), the cycle presented in Chapter2, is to be regarded as the cycle of interest, i.e an ideal Otto cycle with the additional gas exchange process.
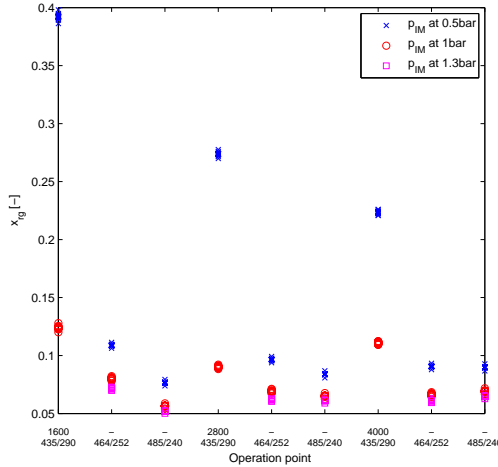
Figure 6.3. x_{rg} plotted for the different operation points, where the three different values of p_{IM} have been marked as shown in the figure. With a low intake pressure and large valve overlap, the amount of residal gas is vastly affected. (The horizontal axis has two different rows, the first row marks the RPM and the second row marks the valve setting. The '-' sign is used if the RPM does not change from the previous operation point.)

temperatures change as the initial conditions alter, results and conclusions can either be verified or concluded.

6.2.2 V_c

From Table 6.1 it is shown that an increased V_c will result in:
a decreased PP and $\dot{m}_{air}$, PPP will move further away from TDC (i.e increase) and an increased of both $T_{Av,Exh}$ and x_{rg}. The effect that V_c has on these quantities can all be summarised into one quantity. That quantity is x_{rg}.

With an increase of V_c, x_{rg} will increase. Hence x_{fm} will decrease and therefore less energy (fresh mixture has $\lambda = 1$ (normalized stochiometric)) for combustion. If x_{rg} would be 100%, then PP would be the result of compression. Thus, with a greater amount of residual gas, PP will decrease.

With an increase of V_c, the compression ratio, r_c[4], will decrease. Thus, the rise of cylinder pressure will be less rapid and more flat, i.e the peak pressure will occur at a later crank angle. (i.e the rate of at which the volume in the cylinder increase after TDC, will be more rapid with a higher compression than a cycle with a lower compression ratio.) Therefore the pressure increase will be greater and occur earlier than with a greater clearance volume.

---

[4]i.e $r_c = \frac{V_c+V_d}{V_c}$

Also as discussed above, the amount of residual gas will decrease as V_c decreases. Hence, the pressure will increase further.

The decreased compression will also yield a smaller volume for expansion. (i.e the volume where the expansion of the gas will be transferred to displacement of the piston.) This implies that the exhaust temperature will increase[5].

Lastly the fact that $\dot{m}_{air}$ decreases, i.e if x_{rg} increases then there will be less x_{fm}. Hence there will be less air in the cylinder and therefore a lower $\dot{m}_{air}$.

With the use of an ideal Otto cycle, an expression for the residual gas mass fraction has been derived, see Equation 2.7. As V_c increases in Equation 2.7 this will lead to an increase of x_{rg}. Although with an increase of V_C, T_{exp} (i.e the temperature at the end of expansion) will also increase. The reason for this is that the burned gas will be let to expand in a smaller volume. Hence, its heat transfer to the expansion process will be lower. There will be a lot of heat, or energy, left in the burned gas upon the begining of the blowdown. This will increase T_{exp} (see Chapter 2), which in turn will increase the exhaust temperature (the gas flowing out of EV is warmer therefore the exhaust gas temperature will be higher).

The impact that V_c has on x_{rg} could therefore explain why V_c has the affect it has as shown in Table 6.1.

An extended version of Table 6.1 and V_c, will not be presented. This is because of that the general behaviour from V_c is described by Table 6.1.

6.2.3   *Phasing*

The parameter $Phasing$ will set the crank angle at which the combustion should be initiated[6]. $Phasing$ was changed as the all the other parameters, $\pm$ 5% from its nominal value. The nominal value for $Phasing$ is $10°$ ATDC. Despite the small change in $Phasing$ and $Duration$, the change is significant, as seen in Table 6.1. Therefore they are both highly significant parameters for PP and PPP.

According to Table 6.1, an increased $Phasing$ will lead to:
a decrease in PP and an increase in both PPP and $T_{Av,Exh}$.

With an increase of $Phasing$, a decrease in PP is fully understandable. This is from the fact that when the combustion is initiated the volume is greater (with an increase in $Phasing$) and therefore the pressure will drop, hence PPP will also increase (i.e move towards BDC). Also, with the increase of $Phasing$, a greater mass of fuel will burn at later crank angles, i.e the expansion from the burned gases, occurs at a greater volume. Thus, the utilization of the energy in the burned gas, will decrease.

---

[5]In fact a higher T_{exh} will decrease m_{rg}, hence x_{rg} decreases.
[6]i.e at which crank angle 50% of total mass(m_{tot}) has burned, i.e at which crank angle the combustion will commence ($Duration$ is unchanged)

This will yield a higher exhaust gas temperature. This is because of that there is still a lot of heat, i.e energy, left in the exhaust gas at EVO[7]. (The change of $Phasing$ is comparable to spark advance, as a part of knock control, see e.g. [6].)

The result yielded in Table 6.1, represent the general behaviour for $Phasing$ at 1600 RPM. Therefore there is no need for an extended version of that table.

6.2.4 $Duration$

According to Table 6.1 an increase in $Duration$ will cause a decrease in both PP and PPP.
$Duration$ is simply burn duration, i.e for how long the gas will burn during combustion. $Phasing$ is still set at 10° ATDC.(i.e at 10° ATDC 50% of the mass should have been burned.) Therefore if $Duration$ is set to 60 degrees, the start of the combustion will be at $30 - 10 = 20°$ degrees BTDC and it will end at $30 + 10 = 40°$ ATDC. Therefore a change in $Duration$ could be seen as spark adjustment, just as $Phasing$.

During simulation the combustion is perfect, i.e every air/fuel mixture will burn. Nearly all (99%[8]) of the fuel will burn during combustion.

From the fact that an increase of $Duration$, yields longer burn duration, the exhaust temperature will increase. If the gas is let to combust during a greater period of time then it will, in extreme cases, still burn at EVO. If the mixture is let to burn during a longer period of time then the same amount of energy is released but under a longer period of time. Hence this will decrease PP. The combustion can not take fully advantage of the increased cylinder pressure during compression. Therefore PPP will also decrease. This is from the fact that PP must be developed somewhat closer to TDC, were it can make as much use of compression as possible.

As with $Phasing$, the general behaviour for $Duration$ is represented by Table 6.1.

6.2.5 A_{EV}

A greater valve area will increase the effective flow area. Table 6.1 reveals that an increased valve area will:
decrease PP, PPP, $\dot{m}_{air}$ and increase x_{rg}.

There is one behaviour that can explain the results given above, which is the increased amount of residual gas. With a greater valve area there will be more x_{rg}, which will result in less m_{af}. Hence, $\dot{m}_{air}$ will decrease. From the fact that m_{fm} decreases, this implies that less energy will be available for combustion. Hence PP will decrease, i.e there is not enough energy to further increase the cylinder pressure.

---

[7]note that each parameter is changed separately, i.e the burn duration is not affected by a change in $Phasing$
[8]The last percent will burn at EVO.

This will also cause PP to occur at an earlier crank angle, i.e. PPP will decrease.

There is also the fact that with a vast amount of x_{rg}, the mixing temperature between the fresh mixture and residual gas will be higher (c.f Figure 6.6). This will result in a higher gas temperature at the beginning of compression. This will further lower the volumetric efficiency and therefore also effect the amount of energy inducted during the intake phase.

As noted earlier, with a greater valve area the flow through the valve will increase. Thus, both the flow out of EV but also the flow from the exhaust pipe to the cylinder, i.e the backflow. A greater area will increase the backflow, c.f Figure 6.4 .
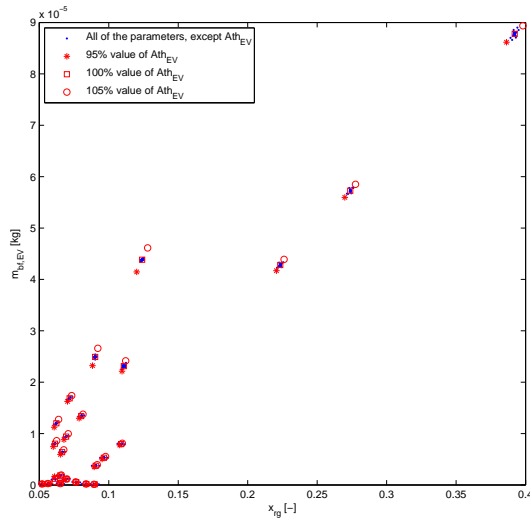
Figure 6.4. Backflow plotted against x_{rg} for all of the parameters, were the altered values of A_{EV} has been marked. As can be seen, the backflow is vastly affected by a change of valve area.

Unlike the parameters discussed sofar, simulations with A_{EV} have provided results that differed from Table 6.1. Those operation points are presented in Table B.1.

As could be noted in Table B.1, there is one interesting operation point for PP, that does not yield the same result as in Table 6.1. The operation point of interest, has a low intake pressure and a normal valve overlap. However, the amount of x_{rg} will still be affected in the same manner as shown in Table 6.1. Thus, the amount of x_{rg} does not decrease at this operation point.

Since the peak pressure does not decrease, even though the inducted energy does so, the reason for an increase of PP must lie elsewhere. Instead, the reason for an increase of PP could be from a reduction of backflow through EV. With this said, the amount of residual gas does not need to decrease, it could be a reduction of the *potential* backflow.

Therefore, the reduction of backflow will yield a less reduction of air charge, i.e the inducted energy is reduced but not as much as it could have been.

Thus, with the increased amount of residual gas, the mixing temperature [9] will increase, c.f Figure 6.6. Since the mixing temperature is increased, the temperature (pressure) at the start of combustion will be higher. Thus, PP will increase.

In Table B.1 there are three operation points that have a different correlation, compared to Table 6.1, between A_{EV} and x_{rg}. These operation points share the same valve setting, which is the smallest valve overlap. With a small overlap the backflow through EV is reduced. The relation between valve overlap and backflow is shown in Figure 6.5 and as can be seen there is a clustering of points for the different valve settings.

With a smaller valve overlap, the time when the two valves are open at the same instant is decreased. Thus, the expansion of exhaust gas into the intake manifold will decrease, i.e backflow will decrease.

There is also another effect that will increase the backflow, which is the timing of a reflection from an exhaust pulse. The origin of a reflection could either be from the exhaust gas that have just been pushed out or from another cylinder´s blowdown.

At these operation points the backflow through EV is minimised (c.f Figure 6.5). Therefore at the small valve overlap the backflow is decreased. Hence reducing the amount of residual gas, and increasing the amount of fresh mixture. Therefore an increase of $\dot{m}_{air}$ will occur. Thus, this will increase the amount of energy for combustion and the exhaust temperature.

6.2.6 T_{Wall}

During simulation the cooling of the wall is treated as an ideal process. Hence the temperature will be the same regardless of what occurs in the cylinder. Therefore, T_{Wall} could be set to a specific value. An increase of T_{Wall} results in, from Table 6.1:
a decrease in PP, PPP, x_{rg} and $\dot{m}_{air}$ while there will be an increase of the exhaust temperature, $T_{Av,Exh}$.

An increase of T_{Wall} will yield less heat transfer (c.f Equation 2.8) between the cylinder wall and the gas located within the cylinder. The heat transfer could in fact be reversed during the start of compression, i.e the gas is heated by the wall. During combustion the gas will become much warmer than T_{Wall}, therefore the heat transfer will be from the gas to the wall. With a higher T_{Wall} the heat transfer during combustion will be lower. Therefore the combustion will take place at a higher temperature.

---

[9]i.e the temperature for the mixture consisting of air/fuel mixture and residual gas, upon the start of compression.
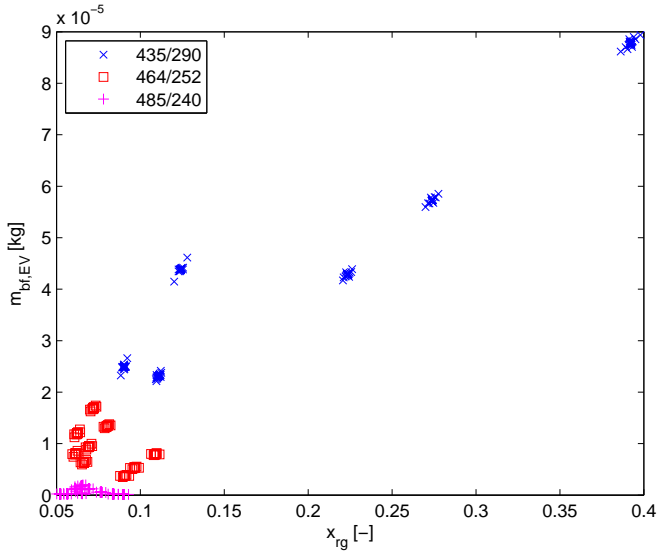
Figure 6.5. Backflow through EV, $m_{bf,EV}$, plotted against x_{rg} and valve setting as shown in figure. As can be seen there is a clustering of points for the different valve settings (i.e. backflow).

Hence, the end gas temperature will be higher, i.e the exhaust gas temperature will be higher.

With a higher temperature the density, ρ, of the gas will decrease. Thus, the same amount of mass will occupy a greater volume. The amount of residual gas (mass) fraction will therefore decrease.

With the increase of T_{Wall} there will also be an increase of T_{fm}. This comes from the fact that both the content and the sorroundings of the cylinder is now warmer. Hence the fresh mixture will be heated. As noted before, the same amount of mass at a higher temperature will occupy a greater volume. Hence, the air mass flow will decrease. Since the air mass flow is decreased, there will be less energy (i.e air/fuel mixture) trapped inside the cylinder upon IVC. Hence, PP will be lower (despite the fact that less energy is lost during combustion for heating of the wall). PPP will therefore occur at an earlier crank angle.

In Figure 6.6, it is shown that an increase of wall temperature gives a lower residual gas mass fraction. The mixing temperature, or T_{Com}, is the mixing temperature between the residual gas and the fresh mixture gas at IVC. Hence, the higher the temperature of residual gas (and mass), the higher the mixing temperature.

 The general behaviour for T_{Wall} is represented in Table 6.1, thus there is no need for an extended version for T_{Wall}.
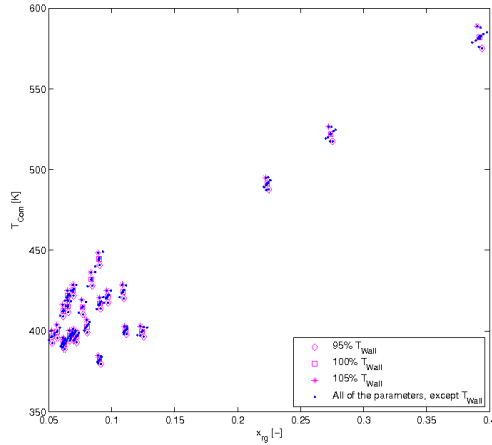
Figure 6.6. The mixing temperature, T_{Com}, is plotted against x_{rg}. The increased, decreased and the nominal value of T_{Wall} has been marked. The increase of T_{Wall} will yield , with virtually the same amount of residual gas, a higher mixing temperature.

6.2.7 A_{IV}

From Table 6.1, the parameter A_{IV} yield a noticable effect on x_{rg}. The recorded x_{rg} at that operation point is well above the limit of $x_{rg} \approx$ 25-30%, where misfire (or dilute misfire) occurs ([4] p.425). Therefore this operation point is not realistic.
Instead, the results from the operation points presented in Table B.2, are of interest. They all yield the same result as the operation point for A_{IV} and x_{rg} presented in Table 6.1.

The behaviour which A_{IV} give rise to can be explained by that an increased of valve area, the backflow through EV will be enhanced. With a larger valve area, the restriction will become less significant. Thus, the mass flow will be less impeded in both directions, both upstreams and downstreams. If the pressure in the intake pipe is less than that of the exhaust gas, there will be an expansion of the exhaust gas into the intake pipe. This backflow will be further enhanced if the valve area is increased. On the other hand, if $p_{IM} > p_{EM}$, the filling/expansion of fresh mixture into the cylinder will be made easier.

Table B.2, show that as the valve overlap decreases, the effect from the change in valve area, decreases. Therefore, the valve area will be of greater importance when the operation point involve a great valve overlap, and therefore a great backflow. From Figure 6.7, a significant backflow through EV will also result in a backflow through IV (i.e a cross flow). Hence, if the backflow through IV would increase, as is the case with a greater valve area (c.f Figure 6.8), then this would enhance the backflow through EV. Therefore as noted in 6.2.5, this would increase the amount of residual gas.
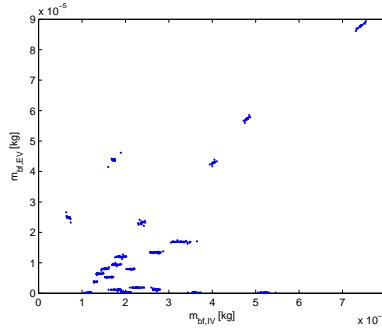
Figure 6.7. $m_{bf,EV}$ plotted against $m_{bf,IV}$. An increase of backflow at EV, will yield the same at IV.

6.2.8 $A_{P,EM}$

The nominal value of $A_{P,EM}$ is $12.8cm^2$ and valve area is $12cm^2$ ($C_d = 0.8$ for the valve area). Therefore a $\pm 5\%$ change in the nominal value is greater than the effective valve area. The valve area will therefore still be the limiting factor, even after the change in $A_{P,EM}$.

According to Table 6.1, an increase in $A_{P,EM}$ will yield a decrease of x_{rg}. With the increase of $A_{P,EM}$, the volume of the exhaust manifold will increase. This increase of volume will lead to slower pressure dynamic. With a slower pressure dynamic, the reflection (created at either the end of the pipe or as the gasflow collide with some other gas that is flowing into the exhaust manifold) will take a longer period of time before it will be apparent at the exhaust valve.

If the reflection is well-timed with IVO, or EVC, (causing the backflow to increase), the residual gas fraction will increase. If the reflection is not well-timed, then it will help the scavenging of the cylinder.

From what is observed in Table 6.1, x_{rg} decreases. Hence, the reflection is not well timed with either IVO or EVC[10]. In Figure 6.9, the reflection at the valve overlap could be seen to, with an increase of $A_{P,EM}$, occur at a later crank angle. Figure 6.9, only represents one of the operating point yielding the results as presented in Table 6.1. The results from the other operation points are presented in Appendix C.1.

The operation points, that is not presented in Table 6.1, yields the same results as the one presented. Thus, an extended table will not provide any new information.

---

[10]As will be noted later, the reflection will at a different rpm or a different valve setting, be timed with EVC, or IVO, and therefore increase the amount of residual gas.
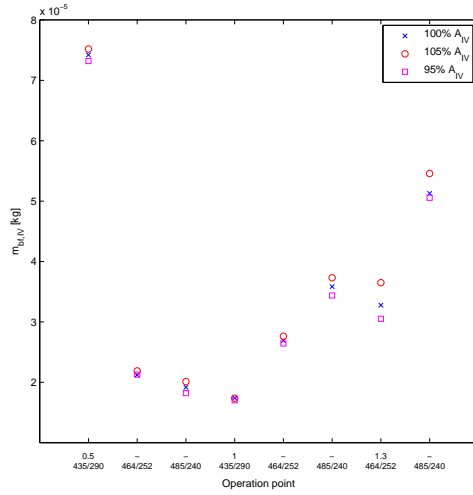
Figure 6.8. $m_{bf,IV}$ plotted for the different operation points involving 1600 RPM. The differences in valve area has been marked as shown in figure. The general behaviour is that the backflow through IV is enhanced by a greater valve area. This holds for every operation point.

6.2.9 $L_{P,EM}$

The same analysis as in 6.2.8, holds for $L_{P,EM}$.

6.2.10 $A_{C,IM}/L_{C,IM}$

Table 6.1, reveal that a change in $A_{C,IM}$ will effect the air mass flow. It could also be witnessed that $L_{C,IM}$ yields the same results. The fact that they yield the same results, implies that their effect on the intake manifold volume, i.e the pressure dynamic, is of considerable value.

A larger volume has a slower pressure dynamics (it is easier to empty a small volume than a large). With a greater volume (and a slower dynamic) more air will be held inside the intake manifold. Therefore the pressure will not decrease as much at IVO. This implies that there will be an increase of $\dot{m}_{air}$.

In Figure 6.10 the effect of a slower pressure dynamic, i.e an increase of $L_{C,IM}$, is shown. The valve setting could also be seen to have a significant impact on the intake pressure.

In appendix, Figure C.4 show the corrensponding figures for $A_{C,IM}$.
The extended version of Table 6.1 for both $A_{C,IM}$ and $L_{C,IM}$, will not be presented since it does not provide any new information.
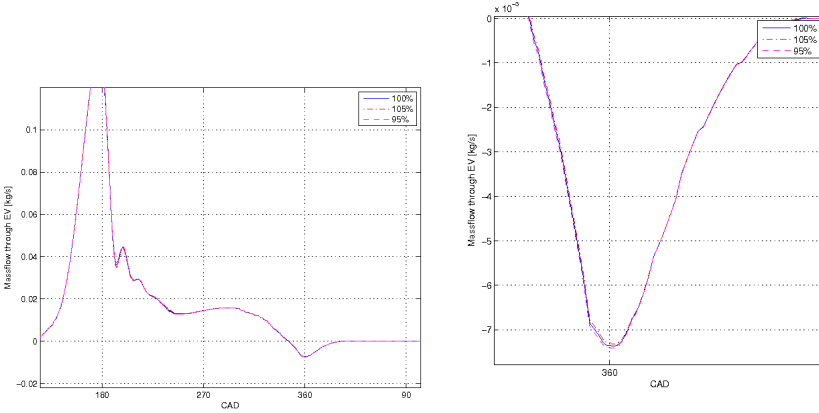
(a) Massflow through EV during gasexchange at 1600 RPM, p_{IM} at 1.3bar and IV/EV 464/252.

(b) An enhancement of Figure 6.9(a), during the valve overlap.

Figure 6.9. Massflow through EV during gasexchange. With a change in $A_{P,EM}$, the timing of reflections will be different. There is a small, but noticeable, reflection in Figure 6.9(b), that occurs at different CAD for the different values of $A_{P,EM}$.

6.3 Results From Other Operation Point Setups

Simulation setups that differ from the setup discussed in previous sections, i.e 1600 RPM, will now be discussed.
For shortening the discussions on results from simulations, only those parameters that does not yield the same behaviour, or order of appearance, as the parameters in Table 6.1, will be investigated. The change of significance must also be significant.

As noted in 6.1.3, each setup for an operation point has a table as Table 6.1. The comparison tables are presented in Appendix A. Each row in the comparison tables should be compared to each other. E.g. the first row of Table A.13 should be compared to the first row of Table A.14, and so forth.

The upcoming sections will only discuss the general behaviour from a different operation point setup, e.g. the different valve settings will all be compared to 1600 RPM. A more comprehensive disccusion is presented in Appendix A.

In 6.2, it was witnessed that some parameters behaved differently with the variation of operation points. The same goes for operation point setups other than 1600 RPM. There were, however, parameters that yielded such resuslt. Those parameters were A_{EV}, A_{IV}, $A_{P,EM}$ and $L_{P,EM}$ and their extended tables are presented in Table B.3, B.4, B.5, B.6, respectively.
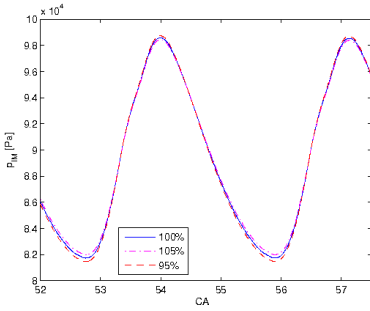
(a) Pressure in intake manifold plotted against crank angle with IV opening as in Figure 6.10(b).
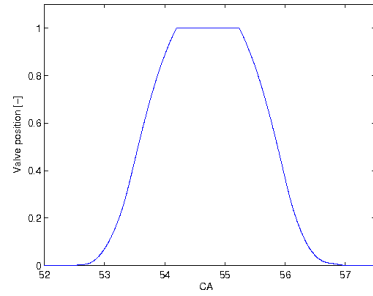
(b) IV opening profile ("0" means valve is closed and "1" means valve is fully open) for IV/EV 435/290
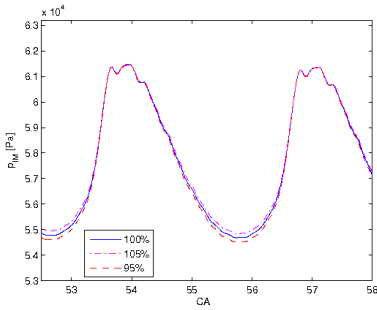

(c) Pressure in intake manifold plotted against crank angle with IV opening as in Figure 6.10(d).
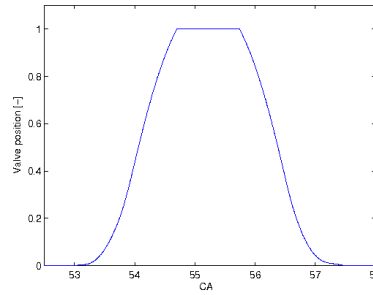
(d) IV opening profile ("0" means valve is closed and "1" means valve is fully open) for IV/EV 464/252.
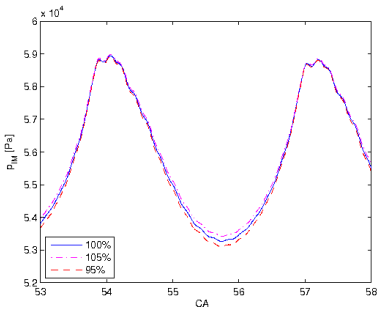
(e) Pressure in intake manifold plotted against crank angle, with IV opening as in Figure 6.10(f).
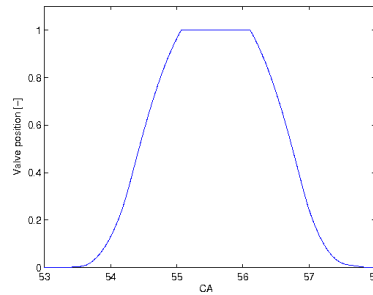
(f) IV opening profile ("0" means valve is closed and "1" means valve is fully open) for IV/EV 485/240

Figure 6.10. The intake manifold pressure at different valve settings and at different lengths of the common intake manifold. The effect from an increase in volume for the intake manifold, on the pressure dynaimcs of the same, is apparent.

6.3.1   Valve Settings 435/290, 485/240 and 464/252

The comparison tables for the simulation results from the different valve settings, IV/EV 435/290, 464/252 and 485/240 compared to 1600 RPM, are presented in Table A.2, A.4 and A.6 respectively.

The general effect from a change of valve overlap (i.e valve setting), is that the backflow, through either of the valve couples, is much affected (c.f Figure 6.2). The effect of a backflow is enhanced if a low intake pressure is present.

Thus, an operation point involving great overlap will yield a vast amount of residual gas. Hence, the parameters that will yield a significant result at low amounts of residual gas, e.g. T_{Wall}, will no longer be significant.

As noted before, an affect on the amount of residual gas can be noticed throughout the complete chain of quantities. The most noticeable effect are from the parameters A_{EV} and T_{Wall}. This is from the fact that was discussed in the paragraph above. The exhaust valve area will clearly become less significant if the valve settings do not allow a backflow of exhaust gas into the intake pipe/manifold.

There are parameters that becomes less significant as the valve overlap increases. The parameter, T_{Wall}, is one of them. This is form the fact that the mixture of air, fuel and residual gas, will have a higher temperature from the begining. This is because of the much warmer residual gas, will heat the air/fuel mixture. Therefore, the effect of a warm cylinder wall, at operation points where a high content of residual gas is present, will be reduced. Thus, as the valve overlap increase, T_{Wall} will become less significant.

Thus, a change in valve overlap will vastly affect the significance of those parameters that is much influenced on the amount of (warm) residual gas.

6.3.2   Low, Part and High Load

The comparison tables for the simulation results from the different engine loads, i.e p_{IM} at 0.5bar, 1bar and 1.3bar, compared to 1600 RPM, are presented in Table A.8, A.10 and A.12 respectively.

A change of intake manifold pressure will, as with valve overlap, have a great influence on the backflow. With a low intake pressure, and a non-zero valve overlap, the backflow through EV and IV, will be enhanced. Thus, with a high intake pressure, this effect will almost be totaly diminished.

The combination of a low (high) intake manifold pressure and small (great) valve overlap, will yield about the same amounts of backflow[11].

---

[11]i.e the same amount of residual gas

Since the backflow is reduced at an increase of p_{IM}, the effect of T_{Wall} will increase (or at least remain unchanged).

With a fix intake pressure instead of a fix engine speed, the pressure dynamics will be enhanced, in each pipe. Thus, pipe lengths/area will become more significant since the emptying and filling of a volume will become faster as both engine speed and intake pressure increases, e.g. $L_{P,EM}$ [12] will become significant.

The general behaviour is that, as the intake pressure increases the amount of residual gas decreases, regardless of valve setting. The effect on pressure dynamics in pipes and manifold will also become more apparent.

6.3.3   Engine Speeds

The comparison tables for the simulation results from the different engine speeds, i.e 2800 RPM and 4000 RPM compared to 1600 RPM, are presented in Table A.14 and A.16 respectively.

The differences between Table A.14 compared to Table A.13 and Table A.16 compared to Table A.15, are few, but significant. One of the significant differences is, the parameter T_{Wall}, that will become less significant at a increase of engine speed. This is because of the heat-transfer process is a time-dependent process, thus the effect of T_{Wall} will decrease. The heat-transfer will have less time for development, thus the heating of the gas from the wall will decrease.

As noted in the section above regarding the increase of pressure dynamics, which are also noticeable at the variation of engine speed. Thus, as stated before, pipe length and area will become more significant.

Also because of the increase of engine speed (i.e 2800 RPM and 4000 RPM compared to 1600 RPM), the mass flow will increase[13]. This will cause a reduction of backflow, and an increase of n_{vol}, this is partly because of the increase of inertia for the gas and that a reflection (since the pressure dynamics are much affected) could be more favourable (i.e a non-existing). Thus, the reduction of backflow will cause valve areas to become less significant.

Thus, with an increase of engine speed the pressure dynamics of pipes/manifolds will become more apparent, hence the formation of reflections will be more important, i.e a length, or area, of a pipe/manifold will become more significant.

---

[12]or $A_{P,EM}$ as they both affect the pressure dynamics for the pipe
[13]less time for filling/emptying the, almost, same amount of mass will yield an increase of mass flow

Chapter 7

Conclusions

This chapter will summarise the results and thoughts that have arisen throughout the work.

7.1   Significant Simulation Results

Following Chapter 6, one could see, not surprisingly, that the operating points play a vital role for the effect of any parameter. A great valve overlap will, in general, with the aid of a low intake pressure, cause a significant amount of residual gas. This behaviour is enhanced if either of the intake or exhaust valve area is increased, or if the timing of a reflection (from the gas flow of exhaust gas) in the exhaust pipe/manifold occurs at the event of IVO or EVC.

It is also noticeable that parameters corresponding to the exhaust side of the engine, are more significant than those on the intake side.

The reason for this may be because of their close connection to the creation of a reflection from the exhaust gases. A reflection is much affected by, e.g. a pipe area or length since it will have a direct effect on the pressure dynamics.

It may also reside from the fact that on the exhaust side, not only is the exhaust gas a highly pressurized gas, but it is also at a much greater temperature than that of the intake side. Thus, the both warn and high pressurized exhaust gas, will have a vast impact on the less warm and, more often than not, less pressurized, air charge.

Furthermore, these effects, are further enhanced if the valve overlap permits an expansion of exhaust gas into the intake pipe.

When one of these two effect occurs, the air charge will be mixed with a gas that is at a much greater temperature. Thus, the temperature (and density) of the air charge will increase, i.e the amount of energy inducted during the intake phase will decrease.

In Table 5.3, the paramters that have had their nominal values altered, are presented. As can be noted in Chapter 6, there are a lot of parameters that never became significant enough to end up in any "Maximum relative difference"-table. The reason for this may be that a change in $\pm 5\%$, were not sufficient to achieve a significant change.

7.2   Comparison

In Chapter 4, some results gathered from simulations, were compared to measuered data provided in [4]. The two results that were used for comparison were the volumetric efficiency simulated over a variety of engine speeds and the instantenous exhaust gas mass flow during the gas exchange process.

The considered mass flow (the exhaust gas mass flow) shared the same overall behaviour as the data provided in [4]. Thus, the model that was used during simulation, for a fluid flowing through a restriction provided accurate results. The model of use was an isentropic and compressible gas flowing through a restriction, see Chapter 4.

However, the magnitude of the exhaust mass flow during the blowdown, from simulation, differed by a factor two, compared to the measured data, in magnitude.

It was shown in Chapter 4, with the aid of the fluid flow model, that it is likely that a (small but significant) difference in gas temperature or valve area (i.e. different valve profiles), will cause an increase of magnitude in the exhaust gas mass flow.

The comparison between the volumetric efficiency showed that the overall efficiency was somewhat lower than the measured data. The reason for this was, as one of the conclusions made from the exhaust gas mass flow, the increase of gas temperature. Despite the drop of efficiency, the validation and simulation data shared the same general behaviour.

7.3   Future Work

As noted before, the valve setting has a clear connection, (correlation), with the amount of residual gas and therefore on the amount of air/fuel mixture. This can be developed for controling the amount of residual gas, i.e. controling the amount of energy inducted into the engine. Thus, securing a stable engine operation and reducing the fuel consumption.

Instead of using the different valve overlaps, that are presented in 5.1.3, it would be interesting to treat the valve overlap as a parameter in itself and adjusting it with some finitesimal value. Furthermore, simulations reagarding a change in valve lift would be interesting.

A more thorough study or analysis of the gas temperature in the cylinder should be made, so that the number of factors affecting the results for the validation against data provided in [4], can be reduced to a minimum.

psPack has the implementations of zero dimensional quantities, with the exception of pressure and etcetera, in pipes. Each pipe is divided into N sections (with N=3 per default), i.e. each pipe has N discrete volume segments. It would be interesting to compare the result of these pipes, e.g. mass flow, with measured data, too see if any further development of these are neccessary or if the number of sections should be increased.

References

[1] Gordon P. Blair. *Design and Simulation of Four-Stroke Engines.* SAE, first edition, 1999.

[2] Lars Eriksson. Thermodynamics for chemical equilibrium unsteady flows, and zero dimensional in-cylinder models. Vehicular Systems, Department of Electrical Engineering, Linköpings Universitet, S-581 83 Linköping, Sweden.

[3] Lars Eriksson. Documentation for the chemical equilibrium program package CHEPP. Technical Report LiTH-R-2298, ISSN 1400-3902, Department of Electrical Engineering, Linköpings Universitet, S-581 83 Linköping, Sweden, 2000.

[4] John B. Heywood. *Internal Combustion Engine Fundamentals.* McGraw-Hill Book Company, first edition, 1988.

[5] Markus Klein. *Single-Zone Cylinder Pressure Modelling and Estimation for Heat Release Analysis of SI Engines.* PhD thesis, Linköpings Universitet, 2007.

[6] Lars Nielsen Lars Eriksson. *Vehicular Systems.* Vehicular Systems, ISY Linköping Institute of Technology, 2006.

[7] Per Öberg and Lars Eriksson. Control oriented gas exchange models for CVCP engines and their transient sensitivity. In *Proceedings of New Trends in Engine Control, Simulation and Modelling*, IFP, Rueil-Malmasison, France, 2006.

[8] Per Öberg et al. A dae formulation and its numerical solution for multi-zone thermodynamic models. Technical report, Department of Electrical Engineering, Linköpings University, 2008.

[9] I.I. Vibe. *Brennverlauf und Kreisprocess von Verbennungsmotoren.* VEB Verlag Technik Berlin, 1970. German translation of the russian original.

[10] G. Woschni. Beitrag zum problem des wärmeüberganges im verbrennungsmotor. Number MTZ No. 26, 1965.

[11] G. Woschni. A universally applicable equation for the instantaneous heat transfer coefficient in the internal combustion engine. Number SAE Technical Paper No. 670931, 1967.

Notation

Abbreviations and nomenclature used in the report.

Nomenclature		Abbreviations	
V	Volume [m^3]	V_c	Clearance Volume
m	Mass [kg]	V_d	Displacement Volume
T	Temperature [K]	T_{Exh}	Temperature in exhaust manifold
H	Enthalpy	T_{Wall}	Temperature Cylinder wall
U	Internal energy	TDC	Top Dead Center
x	Mass fraction	ATDC	After Top Dead Center
v	Velocity [m/s]	BDC	Bottom Dead Center
A	Area [m^2]	PP	Peak Pressure
Q	Heat Transfer [W]	PPP	Peak Pressure Position
$\dot{Q}$	Heat Transfer rate [W/s]	CA	Crank Angle
C_p	Specific heat at constant pressure	EV	Exhaust Valve
C_v	Specific heat at constant volume	IV	Intake Valve
C_p	Mass specific heat at constant pressure	IVO/IVC	Intake Valve Opening/Closing
C_v	Mass specific heat at constant volume	EVO/EVC	Exhaust Valve Opening/Closing
C_d	Discharge coefficient	EM	Exhaust Manifold
η	Efficiency	IM	Intake Manifold
L	Length [m]	P	Pipe (subscript for a parameter)
ρ	Density [kg/m^3]	C	Common (subscript for a parameter)
r_c	Compression ratio	Ath	Area throttle
F_r	Friction coefficient	iMOP	intake Maximum Open Position
		eMOP	exhaust Maximum Open Position
		VVT	Variable Valve Timing
		CVCP	Continous Variable Cam Phasing
		rg	Residual gas
		fm	Fresh Mixture
		af	Air/fuel Mixture
		bf	Backflow
		b	burned
		comb	Combustion
		SI	Spark Ignited
		CI	Compression Ignited

Appendix A

Results From Operation Point Setups Other Than Low RPM

This Appendix presents the simulation results from operation point setups other than 1600 RPM. The discussion regarding the tables presented in this Appendix could be found in 6.3.

A.1 Valve Settings

A.1.1 Intake/Exhaust Valve Setting 435/290

Those parameter that differs from 1600 RPM, compared to the valve setting of IV/EV 435/290, are presented in Table A.2.

Quantity	Parameter	Quotient	RPM	p_{IM}	IV/EV	Ind.
PP	T_{Wall}	0.0099	1600	1.3	485/240	↘
x_{rg}	V_c	0.0852	1600	1.3	485/240	↗
x_{rg}	A_{EV}	0.0654	1600	1	435/290	↗
x_{rg}	T_{Wall}	0.0213	1600	1	435/290	↘
x_{rg}	A_{IV}	0.0150	1600	0.5	435/290	↗
x_{rg}	$A_{P,EM}$	0.0124	1600	1.3	464/252	↘

Table A.1. The simulation results for 1600 RPM that differs from IV/EV 435/290.

PP

By comparing the two Tables A.1 and A.2, one can notice that the parameter T_{Wall} for 1600 RPM has been replaced by $A_{C,IM}$ at IV/EV 435/290. This is from the fact that as the amount of residual gas increase, the effect from T_{Wall} will decrease. The mixture of air, fuel and residual gas, will have a higher temperature from the begining.

Quantity	Parameter	Quotient	RPM	p_{IM}	IV/EV	Ind.
PP	$A_{C,IM}$	0.0050	1600	0.5	435/290	↗
x_{rg}	A_{EV}	0.0654	1600	1	435/290	↗
x_{rg}	$A_{P,EM}$	0.0298	4000	1	435/290	↗
x_{rg}	V_c	0.0260	2800	1	435/290	↗
x_{rg}	$L_{P,EM}$	0.0234	4000	1	435/290	↗
x_{rg}	T_{Wall}	0.0231	2800	1	435/290	↘

Table A.2. The simulation results for IV/EV 435/290 that differs from 1600 RPM.

This is because of the much warmer residual gas will heat ther air/fuel mixture. Therefore, the effect of a warm cylinder wall, at operation points where a high content of residual gas is present, will be reduced. This will cause T_{Wall} to become less significant, as the minimum valve overlap (i.e an operation point with small amount of residual gas) is no longer among the operation points of use.

x_{rg}

There are several differences between the two tables, Table A.1 and Table A.2. The cause of this, could be the correlation between a great valve overlap and x_{rg} as explained in 6.2 and Figure 6.2. The parameter $L_{P,EM}$ has replaced A_{IV}, at x_{rg}. The other parameters have only changed their priority and/or their indication.

For the parameter $A_{P,EM}$, it has gone from a negative to a positive correlation with x_{rg}. This is probably from the cause that was discussed in 6.2.8, which is the timing of a re-flection pulse from the exhaust gas. Thus, if the reflection pulse occurs at the event of EVC, the amount residual gas will increase.

The parameter that have replaced A_{IV}, i.e $L_{P,EM}$, both share the operation point setup of a great valve overlap. But the engine speed and intake pressure is different. Both the intake pressure and engine speed has been increased for the operation point, yielding the greater relative difference for $L_{P,EM}$. With the increase in engine speed and intake pressure, there will be an increased mass flow (c.f Figure A.1). The increased mass flow is probably the cause for the change of parameters. The effect caused by A_{IV} on x_{rg} is that the backflow will increase, with a greater valve area. With an increased intake pressure, the backflow will no longer have the same effect. Hence, A_{IV} will become less significant.

For $L_{P,EM}$ it is the reflections and the increased volume (c.f 6.2.10) that affect x_{rg}. The reflections increase with a higher gasflow as could be seen in Figure A.2. The increased pressure dynamics become more evident at a higher engine speed (Figure A.2(b)) than at a lower engine speed (Figure A.2(a)).

The intake pressure is much affected by the change of $L_{P;EM}$, see Figure A.3.

Because of the shorter pipe, a reflection will occur earlier (shorter pipe, less volume to fill) than a longer pipe. In this case, the reflection pulse will therefore arrive at an earlier crank angle compared to a longer pipe. The reflective pulse is "well"-timed with the opening of the intake valve. Thus, the expansion of exhaust gas into the intake pipe will increase. With the increased mass flow into the intake pipe, the pressure in the intake manifold/pipe will increase. The increased backflow, will decrease the amount of fresh mixture that could be inducted during the intake phase. The amount of residual gas will therefore increase. The formation of a reflection is highly dependent on the length of the pipe. In this case it occurs at right (or wrong) moment.

The pressure build-up in Figure A.3, that is noted at CA 52.8–54, occurs when a different cylinder has finished its intake phase and is closing its IV. The mass flow will cease and there will be a pressure buildup in the intake manifold.
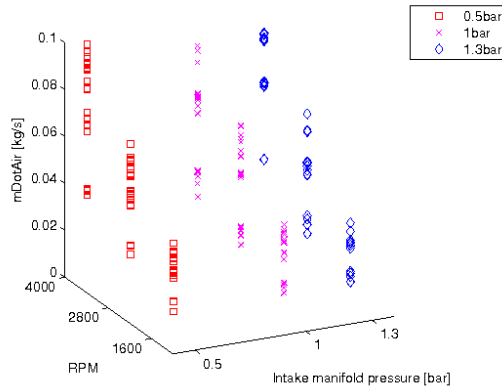
Figure A.1. $\dot{m}_{air}$ plotted against engine speed and p_{IM}. The different intake pressures have been marked as shown in figure. The air mass flow can be seen to increase with engine speed.

A.1.2 Intake/Exhaust Valve Setting 464/252

When comparing Table A.3 with Table A.4, the same parameters for PP, PPP and $\dot{m}_{air}$ are present in both tables. But for $T_{Av,Exh}$ and x_{rg} there are both new parameters and the order of appearance among parameters change, i.e a change in the relative difference.

$T_{Av,Exh}$

Whilst the valve overlap causing the greatest amount of backflow through EV, c.f Figure 6.2, is not being used, the effect of a change in exhaust valve area will therefore become less significant.
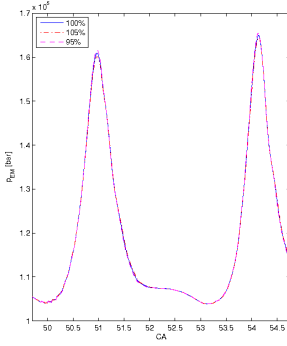
(a) p_{EM} at 1600rpm, IV/EV 435/290 and p_{im} at 1bar, plotted against CA.
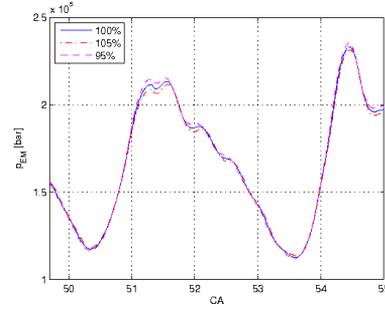
(b) p_{EM} at 4000rpm, IV/EV 435/290 and p_{im} at 1bar, plotted against CA
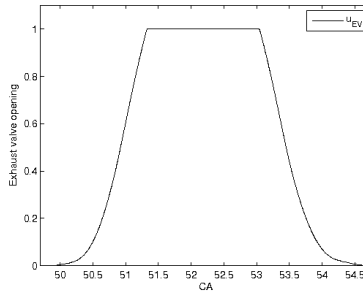
(c) EV profile ("0" means valve is closed and "1" means valve is fully open.) for IV/EV 435/290.

Figure A.2. The exhaust manifold pressure at different engine speeds where the value of $L_{P,EM}$ has been changed by $\pm 5\%$. Figure A.2(a) and Figure A.2(b), share the same valve setting and are both plotted during the gas exchange process. The impact of an increased engine speed for the pressure dynamics in the exhaust manifold is apparent. The change in pipe length could be noted, but the focus lies on the increased pressure dynamics.
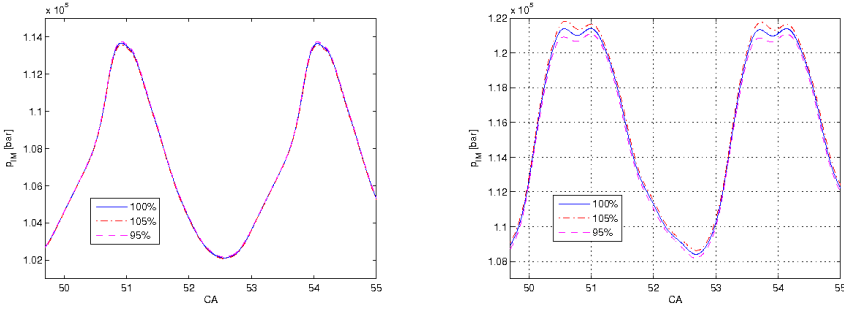
(a) p_{IM} at 1600rpm, IV/EV 435/290 and p_{im} at 1bar, plotted against CA.

(b) p_{IM} at 4000rpm, IV/EV 435/290 and p_{im} at 1bar, plotted against CA

Figure A.3. The intake manifold pressure at different engine speeds where a variation of $L_{P,EM}$ has been made. The valve setting is shown in Figure A.2(c),(IV/EV 435/290). It can be noted that the intake pressure is much affected by a change of $L_{P,EM}$.

Quantity	Parameter	Quotient	RPM	p_{IM}	IV/EV	Ind.
PP	A_{EV}	0.0100	1600	1	435/290	↘
PP	T_{Wall}	0.0099	1600	1.3	485/240	↘
PPP	V_c	0.7656	1600	0.5	435/290	↗
PPP	$Phasing$	0.7339	1600	1.3	485/240	↗
PPP	A_{EV}	0.1019	1600	0.5	435/290	↘
PPP	T_{Wall}	0.0818	1600	0.5	435/290	↘
$T_{Av,Exh}$	A_{EV}	0.0045	1600	0.5	435/290	↘
$T_{Av,Exh}$	$Duration$	0.0021	1600	1.3	485/240	↗
x_{rg}	T_{Wall}	0.0213	1600	1	435/290	↘
x_{rg}	A_{IV}	0.0150	1600	0.5	435/290	↗
x_{rg}	$A_{P,EM}$	0.0124	1600	1.3	464/252	↘
$\dot{m}_{air}$	A_{EV}	0.0226	1600	0.5	435/290	↘
$\dot{m}_{air}$	T_{Wall}	0.0134	1600	1.3	485/240	↘
$\dot{m}_{air}$	V_c	0.0071	1600	0.5	435/290	↘
$\dot{m}_{air}$	$A_{C,IM}$	0.0067	1600	0.5	435/290	↗
$\dot{m}_{air}$	$L_{C,IM}$	0.0067	1600	0.5	435/290	↗

Table A.3. The simulation results for 1600 RPM that differs from IV/EV 464/252.

x_{rg}

The parameter $L_{P,EM}$ has increased its significance and is now present in Table A.4. The parameter that comes second to $L_{P,EM}$ is $A_{P,EM}$. Therefore, the volume of the exhaust pipe/manifold plays a vital role. As discussed in Chapter 6, a change of either length or area for the pipe/manifold, the pressure dynamics will be effected.

Quantity	Parameter	Quotient	RPM	p_{IM}	IV/EV	Ind.
PP	T_{Wall}	0.0081	1600	1.3	464/252	↘
PP	A_{EV}	0.0050	1600	1.3	464/252	↘
PPP	$Phasing$	0.7269	1600	1.3	464/252	↗
PPP	V_c	0.6855	1600	0.5	464/252	↗
PPP	T_{Wall}	0.0562	1600	0.5	464/252	↘
PPP	A_{EV}	0.0218	2800	1.3	464/252	↘
$T_{Av,Exh}$	$Duration$	0.0021	1600	1.3	464/252	↗
$T_{Av,Exh}$	A_{EV}	0.0010	4000	1.3	464/252	↘
x_{rg}	$L_{P,EM}$	0.0150	2800	1.3	464/252	↘
x_{rg}	$A_{P,EM}$	0.0148	2800	1.3	464/252	↘
x_{rg}	A_{IV}	0.0137	1600	0.5	464/252	↗
$\dot{m}_{air}$	T_{Wall}	0.0121	1600	1.3	464/252	↘
$\dot{m}_{air}$	A_{EV}	0.0079	1600	1.3	464/252	↘
$\dot{m}_{air}$	$A_{C,IM}$	0.0054	4000	0.5	464/252	↗
$\dot{m}_{air}$	$L_{C,IM}$	0.0054	4000	0.5	464/252	↗
$\dot{m}_{air}$	V_c	0.0046	1600	1.3	464/252	↘

Table A.4. The simulation results for IV/EV 464/252 that differs from 1600 RPM.

Thus, the timing of a reflective pulse from the exhaust flow, will with this valve setting aid the scavenging process. Hence, decreasing the residual gas mass fraction.
The parameter T_{Wall}, becomes less significance in Table A.4. This is because of that the heat transfer is a time-dependent process and with an increase of engine speed, this effect will decrease (processes that occurs quickly will be favored at high engine speeds). T_{Wall} will therefore become less significant at higher engine speeds.

$\dot{m}_{air}$

As noted in the piece regarding $T_{Av,Exh}$, the parameter A_{EV} was seen to become less significant because of the valve setting. This is also noticeble for $\dot{m}_{air}$. For $\dot{m}_{air}$, the parameter A_{EV} has decreased its significancy from 2.26% till 0.79%, i.e a decrease of 65%. The reason for this is the correlation between backflow and valve overlap. With this valve setting the valve overlap is shortened. Hence, the exhaust gas cannot expand into the intake pipe. Therefore, the air mass flow will decrease when there is exhaust gas flowing into the intake pipe. Thus, with a smaller valve overlap, this effect is reduced. The operation point that will give the greatest effect, is the one yielding the maximum relative difference for 1600rpm (and A_{EV}), see Table A.3.

A.1.3 Intake/Exhaust Valve Setting 485/240

For the comparison between simualtion results from 1600rpm and IV/EV 485/240 the Tables A.5 and A.6 should be compared.

The valve setting IV/EV 485/240 has the shortest valve overlap (c.f Figure 5.1). Thus, as noted earlier, those parameters that will help the expansion of exhaust gas into the intake pipe during the gas exchange process, will become less significant. This could be noticed by comparison of the two tables (Table A.5 and A.6) and the parameter A_{EV}.

Quantity	Parameter	Quotient	RPM	p_{IM}	IV/EV	Ind.
PP	A_{EV}	0.0100	1600	1	435/290	↘
PP	T_{Wall}	0.0099	1600	1.3	485/240	↘
PPP	V_c	0.7656	1600	0.5	435/290	↗
PPP	$Phasing$	0.7339	1600	1.3	485/240	↗
PPP	A_{EV}	0.1019	1600	0.5	435/290	↘
PPP	T_{Wall}	0.0818	1600	0.5	435/290	↘
$T_{Av,Exh}$	A_{EV}	0.0045	1600	0.5	435/290	↘
$T_{Av,Exh}$	$Duration$	0.0021	1600	1.3	485/240	↗
x_{rg}	A_{IV}	0.0150	1600	0.5	435/290	↗
x_{rg}	$A_{P,EM}$	0.0124	1600	1.3	464/252	↘
$\dot{m}_{air}$	A_{EV}	0.0226	1600	0.5	435/290	↘
$\dot{m}_{air}$	T_{Wall}	0.0134	1600	1.3	485/240	↘
$\dot{m}_{air}$	V_c	0.0071	1600	0.5	435/290	↘
$\dot{m}_{air}$	$A_{C,IM}$	0.0067	1600	0.5	435/290	↗
$\dot{m}_{air}$	$L_{C,IM}$	0.0067	1600	0.5	435/290	↗

Table A.5. The simulation results for 1600 RPM that differs from IV/EV 485/240.

Quantity	Parameter	Quotient	RPM	p_{IM}	IV/EV	Ind.
PP	T_{Wall}	0.0099	1600	1.3	485/240	↘
PP	$A_{C,IM}$	0.0046	4000	0.5	485/240	↗
PPP	$Phasing$	0.7339	1600	1.3	485/240	↗
PPP	V_c	0.6776	1600	1	485/240	↗
PPP	T_{Wall}	0.0551	1600	0.5	485/240	↘
PPP	A_{EV}	0.0079	4000	1.3	485/240	↘
$T_{Av,Exh}$	$Duration$	0.0021	1600	1.3	485/240	↗
$T_{Av,Exh}$	A_{EV}	0.0016	1600	1.3	485/240	↗
x_{rg}	$A_{P,EM}$	0.0121	2800	1.3	485/240	↘
x_{rg}	$L_{P,EM}$	0.0112	4000	1.3	485/240	↘
$\dot{m}_{air}$	T_{Wall}	0.0134	1600	1.3	485/240	↘
$\dot{m}_{air}$	$A_{C,IM}$	0.0068	4000	0.5	485/240	↗
$\dot{m}_{air}$	$L_{C,IM}$	0.0068	4000	0.5	485/240	↗
$\dot{m}_{air}$	V_c	0.0048	4000	1.3	485/240	↘
$\dot{m}_{air}$	A_{EV}	0.0038	4000	1.3	485/240	↘

Table A.6. The simulation results for IV/EV 485/240 that differs from 1600 RPM.

PP

For PP, the parameter A_{EV} will become less significant. The reason for this has already been discussed in the piece above.

The parameter that replaces A_{EV} is $A_{C,IM}$. With an increase $A_{C,IM}$, the pressure dynamics will become less rapid. Thus, the pressure in the intake manifold will be higher throughout the intake phase. Hence, the cylinder pressure at IVC will higher, and therefore the amount of inducted energy during the intake phase will be greater. This will yield a higher PP. This could be seen in Figure A.4.
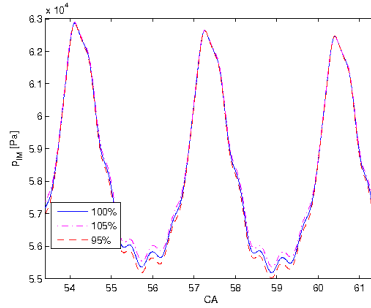
Figure A.4. p_{IM} plotted against CA, with the effect of a change in $A_{C,IM}$ marked as shown in the figure. The increased pressure dynamics in the manifold is apparent as the volume of the same, is varied.

PPP

The shortened valve overlap is also evident for A_{EV} at PPP. The significance for A_{EV} decreases from 0.1019 degrees to 0.0079 degress, an approximate decrease of 92%. This is because of the decreased effect that A_{EV} has on the backflow at a small valve overlap.

$T_{Av,Exh}$

For $T_{Av,Exh}$ the parameters $Duration$, A_{EV} switch places in terms of significance. This is for the same reason as spoken for in the piece above. As the valve overlap decreases, the effect of a change in A_{EV} will become less significant.

x_{rg}

Whilst the great overlap is no longer among the "allowed" operation points, the parameter A_{IV} will become less significant for x_{rg}. A greater intake valve will at a large valve overlap (also, not a necessity but the effect of a backflow will be greatly increased with a low intake pressure) aid the backflow that occurs from the cylinder to the intake pipe. (c.f the case with a greater exhaust valve and a large valve overlap.)

The backflow has a great impact on x_{rg}. Therefore A_{IV} will become less signifant for for x_{rg}, as shown in Table A.6. Instead of A_{IV}, $L_{P,EM}$ (or $A_{P,EM}$) has taken its place. (As mentioned a couple of times before both $L_{P,EM}$ and $A_{P,EM}$ have the same effect on the volume and therefore on the pressure dynamics.)

$\dot{m}_{air}$

The same thing, as with the valve setting IV/EV 464/252, occurs between $\dot{m}_{air}$ and the parameter a_{EV}. The same explanation given in A.1.2, holds.

A.2 Load Settings

A.2.1 Low Load

Overall, a low intake pressure favour the backflow through IV (and also through EV c.f Figure 6.7). Hence, x_{rg} will be higher at a low intake pressure.

By comparison of Table A.7 and Table A.8, only a few differences could be noted.

Quantity	Parameter	Quotient	RPM	p_{IM}	IV/EV	Ind.
PP	T_{Wall}	0.0099	1600	1.3	485/240	↘
x_{rg}	T_{Wall}	0.0213	1600	1	435/290	↘
x_{rg}	A_{IV}	0.0150	1600	0.5	435/290	↗

Table A.7. The simulation results for 1600 RPM that differs from 0.5bar.

Quantity	Parameter	Quotient	RPM	p_{IM}	IV/EV	Ind.
PP	$A_{C,IM}$	0.0050	1600	0.5	435/290	↗
x_{rg}	A_{IV}	0.0206	4000	0.5	435/290	↗
x_{rg}	T_{Wall}	0.0166	1600	0.5	485/240	↘

Table A.8. The simulation results for 0.5bar that differs from 1600 RPM.

PP

The comparison of Table A.7 and Table A.8, show that T_{Wall} has become insignificant for PP, thus T_{Wall} make less of an effect at a low intake pressure.(The operation point in Table A.7 yielding the most significant change, has the smallest valve overlap and a high intake pressure)

With a low intake pressure there will be a great amount of residual gas, c.f Figure 6.3 and Figure 6.2. With a low intake pressure, the gas in the cylinder will expand into the intake.

This expansion will be further enhanced by a great valve overlap.

Thus, with a small valve overlap and a high intake pressure, the amount of residual gas will be reduced. The temperature of the air/fuel mixture is highly correlated with both the temperature of the cylinder wall (the surroundings) and the residual gas (the content).

With small quantities of (high temperature) residual gas, the mixing temperature between the fresh mixture and residual gas will be lower than that of a operation point with greater quantity of residual gas (c.f Figure 6.6).

Hence, the effect of an increased T_{Wall} will decrease for those operation points which has a vast amount of residual gas (c.f Figure 6.3 or Figure 6.2). The heating of the fresh mixture will at those operation points, be caused by the much warmer residual gas. But at small quantities of residual gas, the heating will be caused by the cylinder wall. Thus, at those operation points where there are small quantities of residual gas, the temperature of the cylinder wall will be more significant.

x_{rg}

For x_{rg}, the parameter A_{IV} has increased its significance. From Table B.4 it is clear that with a large valve overlap, the effect of an increased valve area correlates in the positive direction with an increase of the engine speed. This effect is reduced as the overlap decreases. Thus, the low intake pressure and valve overlap, with the greater valve will aid the backflow, or expansion, of exhaust gas into the intake pipe/manifold, see Figure A.5.
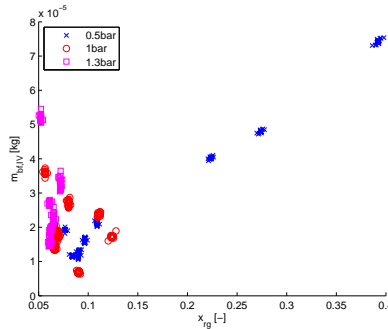
Figure A.5. $m_{bf,IV}$ plotted against x_{rg}, where the values of p_{IM} has been marked. It can be noted that there is a clustering of points for the different intake pressures.

A.2.2   Part Load

With the comparison of the Table A.9 and Table A.10, it is clear that the results from 1 bar, does not involve any radical changes among parameters compared to the results from 1600 RPM.

Quantity	Parameter	Quotient	RPM	p_{IM}	IV/EV	Ind.
PPP	V_c	0.7656	1600	0.5	435/290	↗
PPP	$Phasing$	0.7339	1600	1.3	485/240	↗
PPP	A_{EV}	0.1019	1600	0.5	435/290	↘
PPP	T_{Wall}	0.0818	1600	0.5	435/290	↘
x_{rg}	T_{Wall}	0.0213	1600	1	435/290	↘
x_{rg}	A_{IV}	0.0150	1600	0.5	435/290	↗
x_{rg}	$A_{P,EM}$	0.0124	1600	1.3	464/252	↘
$\dot{m}_{air}$	V_c	0.0071	1600	0.5	435/290	↘
$\dot{m}_{air}$	$A_{C,IM}$	0.0067	1600	0.5	435/290	↗
$\dot{m}_{air}$	$L_{C,IM}$	0.0067	1600	0.5	435/290	↗

Table A.9. The simulation results for 1600rpm that differs from 1bar.

Quantity	Parameter	Quotient	RPM	p_{IM}	IV/EV	Ind.
PPP	$Phasing$	0.7334	1600	1	485/240	↗
PPP	V_c	0.6973	1600	1	435/290	↗
PPP	T_{Wall}	0.0514	1600	1	485/240	↘
PPP	A_{EV}	0.0461	1600	1	435/290	↘
x_{rg}	$A_{P,EM}$	0.0298	4000	1	435/290	↗
x_{rg}	$L_{P,EM}$	0.0234	4000	1	435/290	↗
x_{rg}	T_{Wall}	0.0231	2800	1	435/290	↘
$\dot{m}_{air}$	$A_{P,EM}$	0.0060	4000	1	435/290	↘
$\dot{m}_{air}$	$L_{P,EM}$	0.0048	4000	1	435/290	↘
$\dot{m}_{air}$	V_c	0.0039	1600	1	464/252	↘

Table A.10. The simulation results for 1bar that differs from 1600 RPM.

PPP

The only parameter that undergoes a significant change is A_{EV}. This is because of the increased intake pressure. With a higher intake pressure the backflow through EV, is reduced. Thus, the effect from A_{EV} will become less significant.

x_{rg}

The parameters $A_{P,EM}$ and $L_{P,EM}$ become more significant. This is because of a well timed reflection at this operation point and has already been discussed in A.1.1.

This behaviour (an increase of area or length at the exhaust manifold yielding an increase of x_{rg}) is not the general scenario. This is noticed in Table B.5 and Table B.6.

The general effect should be considered as, that the correlation between the area, or length, at the exhaust manifold and residual gas fraction, is negative. Thus, an increase of area, or length, will yield a decrease in x_{rg}.

This correlation could be explained by the slower pressure dynamics induced by a greater volume. The impact from a greater volume in the exhaust manifold has already been discussed in 6.2.8. The choice of speaking of volume instead of dividing the discussion into length and area, is not length or area specifically, islose connection between the length and area of the exhaust manifold, could be witnessed in Table A.10.

As may also be noticed in the comparison of Table A.9 and Table A.10, the parameter A_{IV} become less significant for PPP. This is from the fact that an increased intake pressure will reduce the backflow through IV (c.f Figure A.5).

$\dot{m}_{air}$

The two parameters $A_{P,EM}$ and $L_{P,EM}$ become more significant for $\dot{m}_{air}$ as the intake pressure is increased. As noted in the piece above regarding PPP, the reflection caused by either of the two paramters, will increase the amount of residual gas. Hence, the air mass flow will decrease. Also as noted in the piece above regarding x_{rg}, the operation point yielding the highest level of significance, has a different indication than more than half of the considered operation points. This, as in the case above, could be explained by the slower pressure dynamic induced by a greater volume. This will lead to less reflections, yielding less backflow and therefore less residual gas. Thus, the mass air flow will increase.

Because of the increased intake pressure, the effect of V_c will decrease. Following the discussion made in 6.2.2, that a change of V_c will affect the residual gas mass fraction. Thus, increasing the intake pressure (and therefore reducing the residual gas mass fraction) the effect of V_c will become less significant.

A.2.3 High Load

From the discussion 6.1.4, the valve setting IV/EV 435/290, with the intake pressure p_{IM} 1.3bar, is not present in Table A.12. By the comparison of the Tables A.11 and A.12, yields only some small differencies. The reason for this is that both 1600 RPM and 1.3bar, yield result where significant changes has been made. They are both "end-values" of the engine speed and intake pressure. It is more likely that such operation will give result that differs from a "normal" operation point.

PP

The parameter A_{EV} becomes less significant as the intake pressure increases. The effect A_{EV} has on PP, is that it will make it easier for a flow of exhaust gas to flow back into the cylinder. With a higher intake pressure this effect is reduced.

Quantity	Parameter	Quotient	RPM	p_{IM}	IV/EV	Ind.
PP	A_{EV}	0.0100	1600	1	435/290	↘
PP	T_{Wall}	0.0099	1600	1.3	485/240	↘
PPP	V_c	0.7656	1600	0.5	435/290	↗
PPP	$Phasing$	0.7339	1600	1.3	485/240	↗
PPP	A_{EV}	0.1019	1600	0.5	435/290	↘
PPP	T_{Wall}	0.0818	1600	0.5	435/290	↘
$T_{Av,Exh}$	A_{EV}	0.0045	1600	0.5	435/290	↘
$T_{Av,Exh}$	$Duration$	0.0021	1600	1.3	485/240	↗
x_{rg}	T_{Wall}	0.0213	1600	1	435/290	↘
x_{rg}	A_{IV}	0.0150	1600	0.5	435/290	↗
x_{rg}	$A_{P,EM}$	0.0124	1600	1.3	464/252	↘
$\dot{m}_{air}$	A_{EV}	0.0226	1600	0.5	435/290	↘
$\dot{m}_{air}$	T_{Wall}	0.0134	1600	1.3	485/240	↘
$\dot{m}_{air}$	$A_{C,IM}$	0.0067	1600	0.5	435/290	↗
$\dot{m}_{air}$	$L_{C,IM}$	0.0067	1600	0.5	435/290	↗

Table A.11. The simulation results for 1600 RPM that differs from 1.3bar.

Quantity	Parameter	Quotient	RPM	p_{IM}	IV/EV	Ind.
PP	T_{Wall}	0.0099	1600	1.3	485/240	↘
PP	A_{EV}	0.0050	1600	1.3	464/252	↘
PPP	$Phasing$	0.7339	1600	1.3	485/240	↗
PPP	V_c	0.6819	1600	1.3	464/252	↗
PPP	T_{Wall}	0.0498	1600	1.3	485/240	↘
PPP	A_{EV}	0.0218	2800	1.3	464/252	↘
$T_{Av,Exh}$	$Duration$	0.0021	1600	1.3	485/240	↗
$T_{Av,Exh}$	A_{EV}	0.0016	1600	1.3	485/240	↗
x_{rg}	$L_{P,EM}$	0.0150	2800	1.3	464/252	↘
x_{rg}	$A_{P,EM}$	0.0148	2800	1.3	464/252	↘
x_{rg}	T_{Wall}	0.0108	1600	1.3	485/240	↘
$\dot{m}_{air}$	T_{Wall}	0.0134	1600	1.3	485/240	↘
$\dot{m}_{air}$	A_{EV}	0.0079	1600	1.3	464/252	↘
$\dot{m}_{air}$	A_{IV}	0.0036	4000	1.3	464/252	↗
$\dot{m}_{air}$	$A_{P,EM}$	0.0028	1600	1.3	464/252	↗

Table A.12. The simulation results for 1.3bar that differs from 1600 RPM.

PPP

The same as with PP and A_{EV}, goes for PPP and A_{EV}. The effect of A_{EV} decreases as the possibilty for a backflow is reduced.

x_{rg}

$A_{P,EM}$, $L_{P,EM}$ become more important as the intake pressure increases. Note that the operation point, with the great valve overlap is not present.

Thus, the well timed reflection that occured at the largest valve overlap, does not exist, instead it is the less rapid pressure dynamic that a greater volume induces, that is noted.

$\dot{m}_{air}$

As was the case with PP and PPP, the effect from A_{EV} is reduced at a higher intake pressure. Therefore the parameter A_{EV} will become less important for $\dot{m}_{air}$.

A.3 Engine Speeds

A.3.1 2800 RPM and 4000 RPM

The two other engine speeds, i.e 2800 RPM and 4000 RPM, yield simulation results that compared to 1600 RPM, are practicly the same. Thus, the analysis can be done simultaneously.

The comparison of simulation results between the two engine speeds, 2800 RPM and 4000 RPM, with 1600 RPM are presented in:
For 1600 RPM compared to 2800 RPM, Table A.13 and Table A.14;
For 1600 RPM compared to 4000 RPM, Table A.15 and Table A.16.
From these tables it is clear that there are some significant changes for PP, $\dot{m}_{air}$ and x_{rg}.

Quantity	Parameter	Quotient	RPM	p_{IM}	IV/EV	Ind.
PP	A_{EV}	0.0100	1600	1	435/290	↘
PP	T_{Wall}	0.0099	1600	1.3	485/240	↘
PPP	A_{EV}	0.1019	1600	0.5	435/290	↘
PPP	T_{Wall}	0.0818	1600	0.5	435/290	↘
x_{rg}	$A_{P,EM}$	0.0124	1600	1.3	464/252	↘
$\dot{m}_{air}$	V_c	0.0071	1600	0.5	435/290	↘
$\dot{m}_{air}$	$A_{C,IM}$	0.0067	1600	0.5	435/290	↗
$\dot{m}_{air}$	$L_{C,IM}$	0.0067	1600	0.5	435/290	↗

Table A.13. The simulation results for 1600 RPM that differs from 2800 RPM.

PP

As the engine speed is increased, the two parameters, A_{EV} and T_{Wall}, yield results where the both of them become less significant.

For A_{EV}, the level of significance decreases since the backflow through EV decreases as the engine speed increases (c.f Figure A.6).

As can be seen in Table B.3, the operation point that yields the maximum relative difference in x_{rg}, comport with the operation point yielding the maximum relative difference for PP in Table A.14. Thus, x_{rg} correlates well with PP.

The operation point consisting of p_{IM} at 1.3bar and IV/EV at 464/252 (2800 RPM), will produce a more significant result. This operation point could be seen in Figure A.6. At this operation point, the backflow is not that great. But in relative terms, it is significant. Thus, the modest increase of backflow at this operation is enough to affect both x_{rg} and PP.

With an increase of engine speed, the piston will more rapidly push the exhaust gas out of the cylinder. Thus, it will be more difficult to change the (flow) direction of the gas. This will lead to a decreased backflow. The effect of an increased engine speed, on the backflow could be seen in Figure A.7(a).
Therefore the parameter A_{EV} will decrease its significance at operation points involving both 2800 RPM and 4000 RPM. Thus, some other parameter will become more important. In Figure A.7, both the $m_{bf,EV}$ and m_{fm} have been plotted as the engine speed varies.
From the fact that the heat transfer process is a time-dependent process, the effect of T_{Wall} will therefore decrease as the engine speed is increased. Thus, T_{Wall} will become less significant at higher engine speeds.

| Quantity	Parameter	Quotient	RPM	p_{IM}	IV/EV	Ind.
PP	T_{Wall}	0.0057	2800	1.3	485/240	↘
PP	A_{EV}	0.0041	2800	1.3	464/252	↘
PPP	T_{Wall}	0.0616	2800	0.5	435/290	↘
PPP	A_{EV}	0.0568	2800	0.5	435/290	↘
x_{rg}	$L_{P,EM}$	0.0150	2800	1.3	464/252	↘
$\dot{m}_{air}$	$A_{C,IM}$	0.0046	2800	0.5	435/290	↗
$\dot{m}_{air}$	$L_{C,IM}$	0.0046	2800	0.5	435/290	↗
$\dot{m}_{air}$	V_c	0.0043	2800	1.3	485/240	↘

Table A.14. The simulation results for 2800 RPM that differs from 1600 RPM.

Quantity	Parameter	Quotient	RPM	p_{IM}	IV/EV	Ind.
PP	A_{EV}	0.0100	1600	1	435/290	↘
PP	T_{Wall}	0.0099	1600	1.3	485/240	↘
PPP	V_c	0.7656	1600	0.5	435/290	↗
PPP	$Phasing$	0.7339	1600	1.3	485/240	↗
PPP	A_{EV}	0.1019	1600	0.5	435/290	↘
PPP	T_{Wall}	0.0818	1600	0.5	435/290	↘
x_{rg}	T_{Wall}	0.0213	1600	1	435/290	↘
x_{rg}	A_{IV}	0.0150	1600	0.5	435/290	↗
x_{rg}	$A_{P,EM}$	0.0124	1600	1.3	464/252	↘
$\dot{m}_{air}$	A_{EV}	0.0226	1600	0.5	435/290	↘
$\dot{m}_{air}$	T_{Wall}	0.0134	1600	1.3	485/240	↘
$\dot{m}_{air}$	V_c	0.0071	1600	0.5	435/290	↘
$\dot{m}_{air}$	$A_{C,IM}$	0.0067	1600	0.5	435/290	↗
$\dot{m}_{air}$	$L_{C,IM}$	0.0067	1600	0.5	435/290	↗

Table A.15. The simulation results for 1600 RPM that differs from 4000 RPM.

Quantity	Parameter	Quotient	RPM	p_{IM}	IV/EV	Ind.
PP	T_{Wall}	0.0049	4000	1.3	485/240	↘
PP	$A_{C,IM}$	0.0046	4000	0.5	485/240	↗
PPP	$Phasing$	0.7255	4000	1.3	485/240	↗
PPP	V_c	0.7139	4000	0.5	435/290	↗
PPP	T_{Wall}	0.0539	4000	0.5	435/290	↘
PPP	A_{EV}	0.0384	4000	0.5	435/290	↘
x_{rg}	$A_{P,EM}$	0.0298	4000	1	435/290	↗
x_{rg}	$L_{P,EM}$	0.0234	4000	1	435/290	↗
x_{rg}	A_{IV}	0.0206	4000	0.5	435/290	↗
$\dot{m}_{air}$	T_{Wall}	0.0081	4000	1.3	485/240	↘
$\dot{m}_{air}$	$A_{C,IM}$	0.0068	4000	0.5	485/240	↗
$\dot{m}_{air}$	$L_{C,IM}$	0.0068	4000	0.5	485/240	↗
$\dot{m}_{air}$	A_{EV}	0.0061	4000	1.3	464/252	↘
$\dot{m}_{air}$	$A_{P,EM}$	0.0060	4000	1	435/290	↘

Table A.16. The simulation results for 4000 RPM that differs from 1600 RPM.

x_{rg}

The effect of a change in T_{Wall} will decrease as the engine speed increases. Therefore, T_{Wall} will become less signficant in Table A.16. The pressure dynamics will increase as the engine speed increase. Thus, a different length or area of the exhaust pipe, will further effect the pressure dynamics.
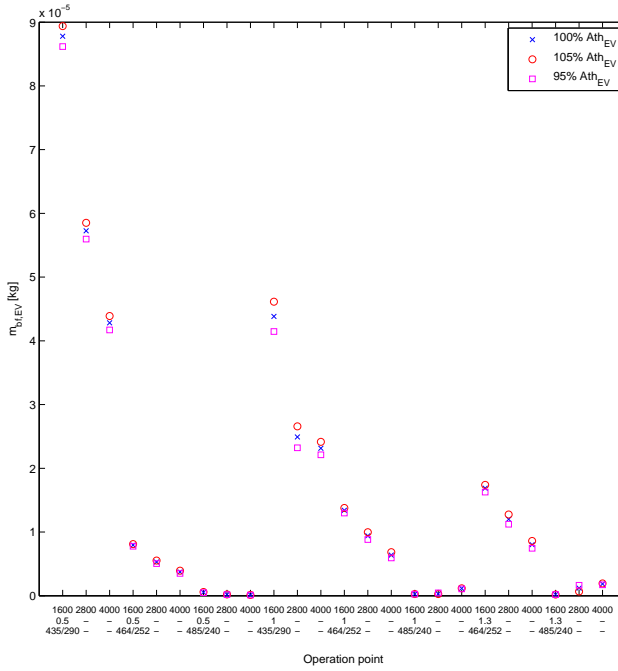
Figure A.6. Mass of backflow through EV plotted for the different operation points. The change of A_{EV} has been marked as the 100% (nominal value), 105% (increased value) and the 95%-value (decreased value). On the horizontal axis the different operation points are shown.

For 2800 RPM (Table A.16), the parameter $A_{P.EM}$ will be replace by $L_{P.EM}$. This however is not a significant change, even though there is a change of parameters. This is because of their common ground in affecting the pressure dynamics, thus it is difficult to separate the behaviour from one of them.

$\dot{m}_{air}$

The differences in $\dot{m}_{air}$ between Table A.15 and Table A.16 are more evident than the comparison of Table A.15 and Table A.16. The parameters V_c and A_{EV} has dropped significantly. The reason for the drop of significance for V_c has been discussed in A.2.2, and still holds.

The reason as for why A_{EV} has become less significant, follows from the discussion in the piece above.
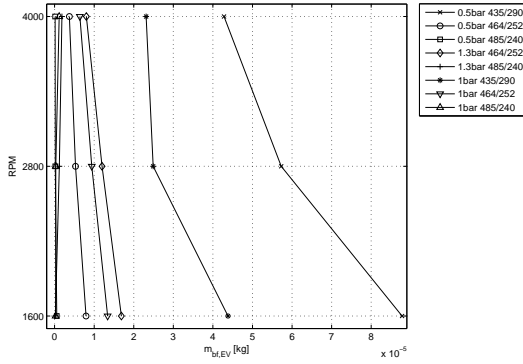
(a) The change of engine speed plotted against the mass of backflow through EV, $m_{bf,EV}$. The nominal value for each parameter has been used, i.e the parameter values are left "unchanged".
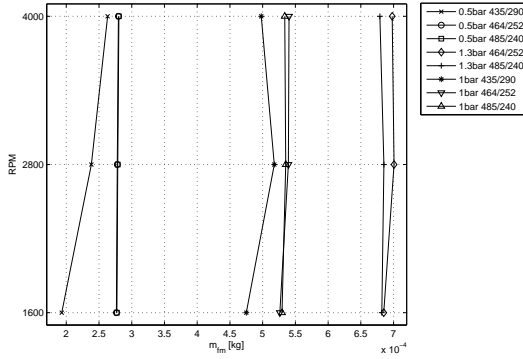
(b) The change of engine speed plotted against mass of fresh mixture (m_{fm}) at IVC. The nominal value for each parameter has been used

Figure A.7. For each and every valid operation point, the effect of a change in engine speed has been plotted against the yielded $m_{bf,EV}$ and m_{fm} at the specific operation point. The change of operation point is presented according the legend in each figure. The $m_{bf,EV}$ and m_{af} could be seen to decrease and increase, respectively, as the engine speed increases.

Appendix B

Extended Tables

This appendix will present the simulation results for those operation points that provided result that where not invariant for operation points. The result needed also to be significant according 6.1.1. The discussion regarding these tables is made in Chapter 6

B.1 Extended tables for 1600 RPM

This section holds the extended tables for 6.2.

Quantity	Parameter	Quotient	RPM	p_{IM}	IV/EV	Ind.
PP	A_{EV}	0.0015	1600	0.5	464/252	↗
PPP	A_{EV}	0.0047	1600	0.5	485/240	↗
PPP	A_{EV}	0.0041	1600	1	485/240	↗
PPP	A_{EV}	0.0037	1600	1.3	485/240	↗
$T_{Av,Exh}$	A_{EV}	0.0016	1600	1.3	485/240	↗
$T_{Av,Exh}$	A_{EV}	0.0016	1600	1	485/240	↗
$T_{Av,Exh}$	A_{EV}	0.0013	1600	0.5	485/240	↗
x_{rg}	A_{EV}	0.0127	1600	1	485/240	↘
x_{rg}	A_{EV}	0.0123	1600	1.3	485/240	↘
x_{rg}	A_{EV}	0.0104	1600	0.5	485/240	↘
$\dot{m}_{air}$	A_{EV}	0.0016	1600	1.3	485/240	↗

Table B.1. The operations points for the parameter A_{EV}, that does not yield the same results as presented in Table 6.1.

Quantity	Parameter	Quotient	RPM	p_{IM}	IV/EV	Ind.
x_{rg}	A_{IV}	0.0150	1600	0.5	435/290	↗
x_{rg}	A_{IV}	0.0137	1600	0.5	464/252	↗
x_{rg}	A_{IV}	0.0106	1600	1	464/252	↗
x_{rg}	A_{IV}	0.0087	1600	1.3	464/252	↗
x_{rg}	A_{IV}	0.0048	1600	1	435/290	↗
x_{rg}	A_{IV}	0.0025	1600	1	485/240	↗
x_{rg}	A_{IV}	0.0025	1600	1.3	485/240	↗
x_{rg}	A_{IV}	0.0017	1600	0.5	485/240	↗

Table B.2. An extended table for the parameter A_{IV}, while the operation point setup with a low engine speed is considered.

B.2 Extended tables for 2800 RPM

Quantity	Parameter	Quotient	RPM	p_{IM}	IV/EV	Ind.
x_{rg}	A_{EV}	0.0528	2800	1.3	464/252	↗
x_{rg}	A_{EV}	0.0453	2800	1	464/252	↗
x_{rg}	A_{EV}	0.0435	2800	1	435/290	↗
x_{rg}	A_{EV}	0.0287	2800	0.5	435/290	↗
x_{rg}	A_{EV}	0.0260	2800	0.5	464/252	↗
x_{rg}	A_{EV}	0.0082	2800	1.3	485/240	↗
x_{rg}	A_{EV}	0.0057	2800	0.5	485/240	↗
x_{rg}	A_{EV}	0.0024	2800	1	485/240	↗

Table B.3. An extended table for the parameter A_{EV}, while the operation point setup with 2800 RPM is considered.

B.3 Extended Tables for p_{IM} at 0.5bar

Quantity	Parameter	Quotient	RPM	p_{IM}	IV/EV	Ind.
x_{rg}	A_{IV}	0.0206	4000	0.5	435/290	↗
x_{rg}	A_{IV}	0.0168	2800	0.5	435/290	↗
x_{rg}	A_{IV}	0.0150	1600	0.5	435/290	↗
x_{rg}	A_{IV}	0.0137	1600	0.5	464/252	↗
x_{rg}	A_{IV}	0.0071	2800	0.5	464/252	↗
x_{rg}	A_{IV}	0.0049	4000	0.5	464/252	↗
x_{rg}	A_{IV}	0.0017	1600	0.5	485/240	↗

Table B.4. An extended table for the parameter A_{IV}, while the operation point setup where a low intake pressure is used.

B.4 Extended tables for p_{IM} at 1.0bar

Quantity	Parameter	Quotient	RPM	p_{IM}	IV/EV	Ind.
x_{rg}	$A_{p,EM}$	0.0298	4000	1	435/290	↗
x_{rg}	$A_{p,EM}$	0.0124–0.0062	All	1	All	↘
x_{rg}	$A_{p,EM}$	0.0040	2800	1	435/290	↗
x_{rg}	$A_{p,EM}$	0.0027	1600	1	485/240	↘

Table B.5. An extended table for the parameter $A_{P,EM}$, while the operation point setup where the intake pressure at 1 bar is used.

Quantity	Parameter	Quotient	RPM	p_{IM}	IV/EV	Ind.
x_{rg}	$L_{p,EM}$	0.0234	4000	1	435/290	↗
x_{rg}	$L_{p,EM}$	0.0127–0.0013	All	1	All	↘

Table B.6. The extended table for the parameter $L_{p,EM}$ regarding the operation point with an intake pressure at 1bar.

Appendix C

# Figures

C.1 Figures for $A_{P,EM}$
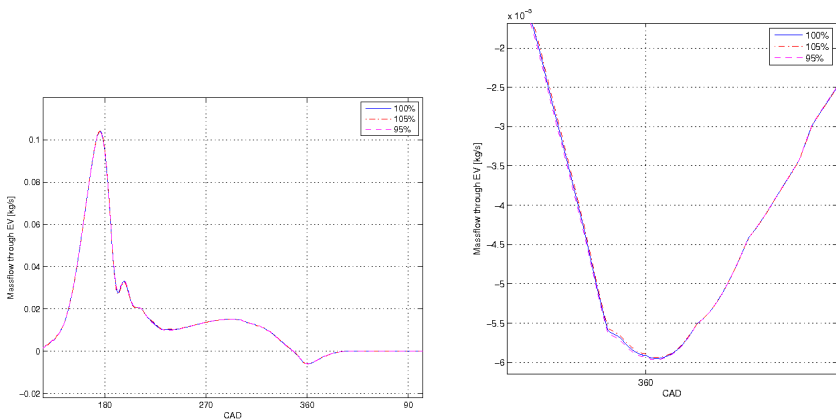
(a) Massflow through EV during gas exchange at 1600rpm, p_{IM} at 1bar and IV/EV 464/252.

(b) An enhancement of Figure C.1(a), at the valve overlap.

Figure C.1. Massflow through EV during gasexchange with IV/EV 464/252. The backflow through EV at the valve overlap has been enhanced. The reflection at the larger pipe area, can be noticed to occur later compared to the smaller piper area.
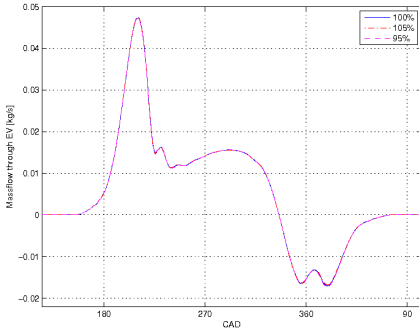
(a) Massflow through EV during gas exchange at 1600rpm, p_{IM} at 0.5bar and IV/EV 435/290.
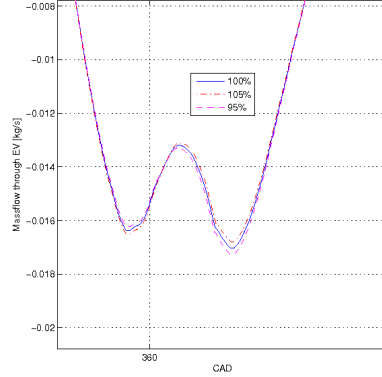
(b) An enhancement of Figure C.2(a), at the valve overlap.
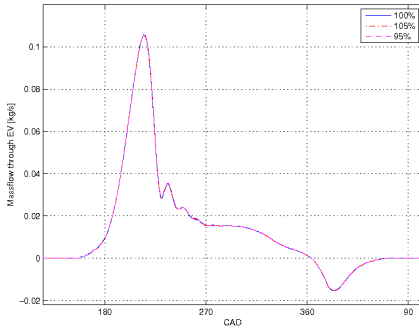
(c) Massflow through EV during gas exchange at 1600rpm, p_{IM} at 1bar and IV/EV 435/290.
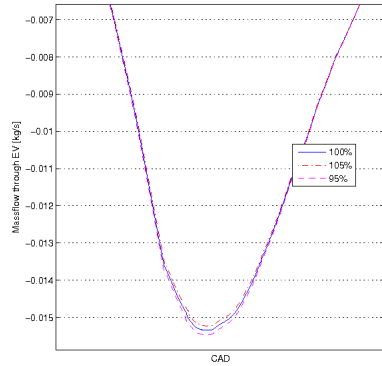
(d) An enhancement of Figure C.2(c), at the valve overlap.

Figure C.2. Massflow through EV during gasexchange with IV/EV 435/290. With the comparison of Figure C.1, the effect of a change in pipe area, timing the reflection differently, at the valve overlap, is much more apparent.
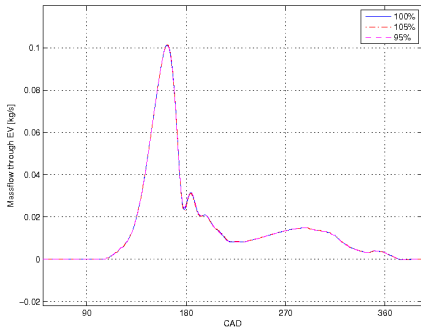
(a) Massflow through EV during gas exchange at 1600rpm, p_{IM} at 1bar and IV/EV 485/240.
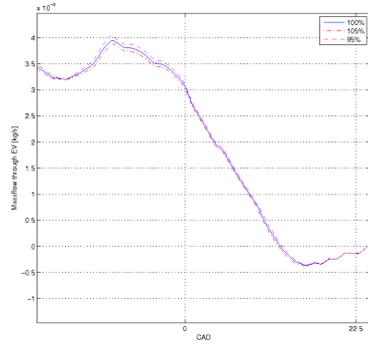
(b) An enhancement of Figure C.3(a), at the valve overlap.
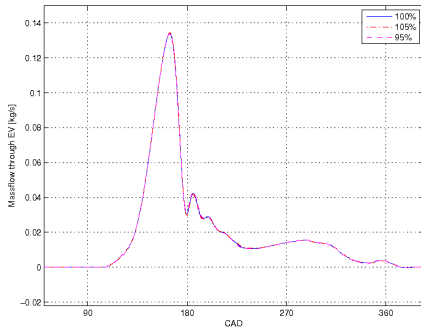
(c) Massflow through EV during gas exchange at 1600rpm, p_{IM} at 1.3bar and IV/EV 485/240.
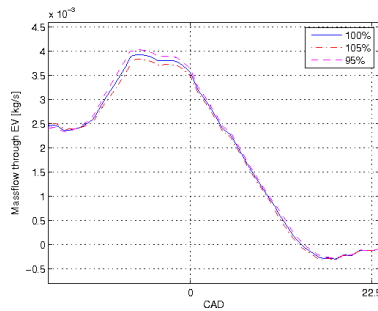
(d) An enhancement of Figure C.3(c), at the valve overlap.

Figure C.3. Massflow through EV during gasexchange with IV/EV 485/240. With the smallest valve overlap, the effect of a late opening and early closing of IV and EV respectively is apparent as an increase in cylinder pressure can be noticed just before IVO. The backflow during the valve overlap is not as significant, comparead to Figure C.1 and Figure C.2

C.2   Figures for $A_{C,IM}$
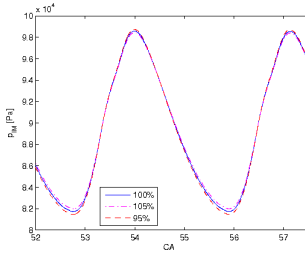
(a) Pressure in intake manifold plotted against crank angle with IV opening as in figure C.4(b).
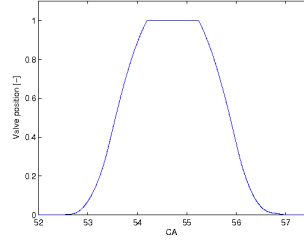
(b) IV opening profile ("0" means valve is closed and "1" means valve is fully open) for IV/EV 435/290
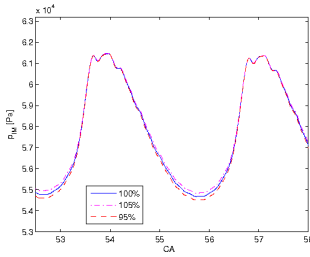
(c) Pressure in intake manifold plotted against crank angle with IV opening as in figure C.4(d).
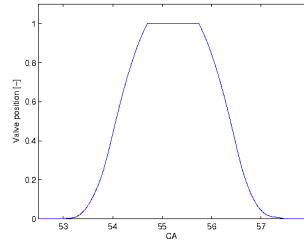
(d) IV opening profile ("0" means valve is closed and "1" means valve is fully open) for IV/EV 464/252.
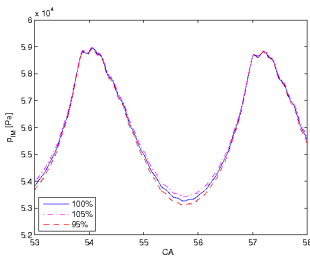
(e) Pressure in intake manifold plotted against crank angle, with IV opening as in figure C.4(f).
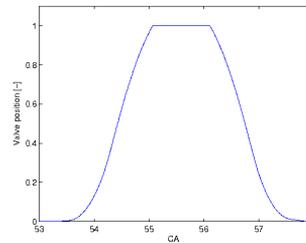
(f) IV opening profile ("0" means valve is closed and "1" means valve is fully open) for IV/EV 485/240

Figure C.4. Intake manifold pressure at different valve settings and at different area of the common intake manifold. The pressure dynamics, i.e the emptying and filling, of the intake manifold, is much affected by a change in $A_{C,IM}$.